Atmospheric iodine, selenium and caesium depositions in France: I. Spatial and seasonal variations

Marine Roulier, Maïté Bueno, Frédéric Coppin, Manuel Nicolas, Yves Thiry, François Rigal, Isabelle Le Hécho, Florence Pannier

Atmospheric iodine, selenium and caesium depositions in France: I. Spatial and seasonal variations

Marine Roulier * [a, b], Maïté Bueno [a], Frédéric Coppin [b], Manuel Nicolas [c], Yves Thiry [d], François Rigal [a, e], Isabelle Le Hécho [a] and Florence Pannier [a].

*corresponding author

[a] CNRS/Univ. Pau & Pays de l'Adour/E2S UPPA, Institut des Sciences Analytiques et de Physico-Chimie pour l'Environnement et les Matériaux, UMR 5254, Avenue du Président Angot, 64000 Pau, France (E-mail addresses: roulier.marine@univ-pau.fr; maite.bueno@univ-pau.fr; florence.pannier@univ-pau.fr; isabelle.lehecho@univ-pau.fr; francois.rigal@univ-pau.fr)

[b] Institute of Radiological Protection and Nuclear Safety (IRSN), PSE-ENV/SRTE/LR2T, CE Cadarache, 13115 Saint Paul les Durance Cedex, France (E-mail addresses : frederic.coppin@irsn.fr)

[c] Office National des Forêts (ONF), Direction forêts et risques naturels, Département recherche, développement, innovation, Boulevard de Constance, 77300 Fontainebleau, France (E-mail address: manuel.nicolas@onf.fr)

[d] Andra, Research and Development Division, Parc de la Croix Blanche, 1-7 rue Jean Monnet, 92298 Châtenay-Malabry Cedex, France (E-mail address: yves.thiry@andra.fr)

[e] Azorean Biodiversity Group, cE3c – Centre for Ecology, Evolution and Environmental Changes, Angra do Heroísmo, Azores, Portugal

Graphical Abstract

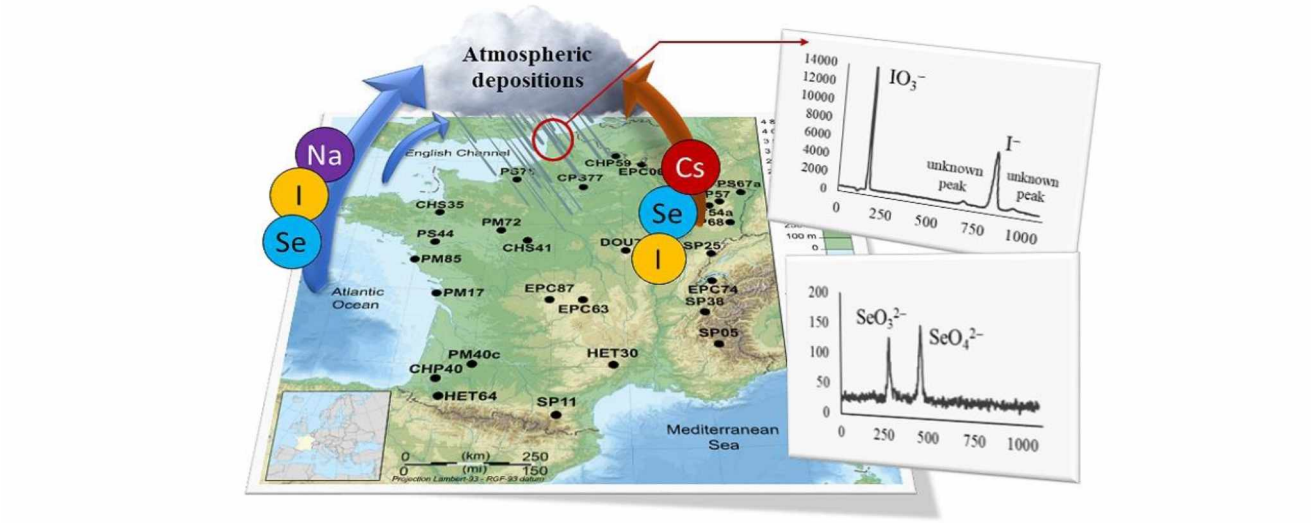

Highlights:

- Spatial distribution and seasonal variations of I, Se and Cs in rains in France
- Annual I, Se and Cs concentrations of: 0.8-2.7 µg L^{-1}; 23-85 and 2.3-13.2 ng L^{-1}
- Common trends for I and Se with relatively homogeneous annual deposition fluxes
- No specific seasonal trend occurred for Cs and Se contrary to I
- On annual average, less than the half of I and Se are inorganic compounds

Abstract

The spatial distribution and seasonal variations of atmospheric iodine (I), selenium (Se) and caesium (Cs) depositions remain unclear and this precludes adequate inputs for biogeochemical models. We quantified total concentrations and fluxes of these elements in rainfalls from 27 monitoring sites in France with contrasted climatic conditions; monthly measurements were taken over one year (starting in 2016/09). Since speciation of I and Se can impact their behaviour in the environment, analysis of their inorganic compounds was also conducted. Our results showed that annual I concentrations in rainfall were much higher than those of Se and Cs (annual means = 1.56, 0.044 and 0.005 μg L^{-1}, respectively). The annual iodine concentrations were highly positively correlated with those of marine elements (i.e. Na, Cl and Mg), involving higher I concentrations under oceanic climate than for transition, continental and mountainous ones. Furthermore, common patterns were found between Se concentrations and both marine and terrestrial components consistent with the various sources of Se in atmosphere. The association of Cs with two anthropogenic components (i.e. NH_4^+ and NO_3^-) used in agriculture supports the hypothesis of its terrestrial origin (i.e. from atmospheric dusts) in rainfall. We found higher rainfall concentrations of I during the warmest months for all climates. However, no specific seasonal trend occurred for Se and Cs. On annual average, rainfall contained mostly unidentified selenium compounds (inorganic Se proportions = 25-54%) and equal proportions of inorganic and unidentified I compounds. Concentrations of iodate were higher under oceanic climate consistent with an iodine marine-origin.

Keywords: Iodine; Selenium; Caesium; Speciation; Rain; Climatic conditions

1. Introduction

Although atmospheric deposits of stable iodine and selenium are known to play a major role in their supply and cycling into the biosphere, data related to stable caesium are very limited. Beyond enrichment of existing data sets, the monitoring of stable isotopes atmospheric deposits allows to understand the long-term behaviour of corresponding radionuclides (i.e ^{129}I, ^{79}Se, ^{137}Cs) that may incorporate the global cycling of their stable analogues. Atmospheric iodine, selenium and caesium are transported and transferred to the Earth's surface with wet and dry depositions. Furthermore, forest ecosystems are particularly sensitive to atmospheric inputs due to the large interacting surface area of the forest canopy, which could influence elemental composition of incoming water during canopy crossing. The current understanding of atmospheric selenium, iodine and caesium interception by tree canopy as a first step of elements recirculation and redistribution to the forest floor is insufficient. To that end, quantifying the spatial distribution and seasonal variations of iodine, selenium and caesium atmospheric depositions onto forest is an important first step.

Most studies about atmospheric deposition of stable iodine indicate that this element in the atmosphere mainly originated from volatilisation from the marine environment (Fuge and Johnson, 2015). Methyl iodide (CH_3I), diiodomethane (CH_2I_2), chloroiodomethane (CH_2ICl), bromoiodomethane (CH_2IBr) and molecular iodine (I_2) are the major sources of marine atmospheric iodine from biological and photochemical pathways (Saiz-Lopez et al., 2012). These compounds would rapidly be photolyzed in the atmosphere to form iodine oxide aerosols (I_2O_5) although significant proportion of iodide and organo-iodine has been reported in marine aerosols (Gilfedder et al., 2007a). Volatilisation of iodine occurs also from terrestrial environment with the emission of molecular iodine and methyl iodide (Fuge and Johnson, 2015). Volcanic emissions have been estimated to be negligible in comparison with marine and terrestrial sources and, coal combustion has been identified as anthropogenic source of

atmospheric iodine that may influence iodine levels in rainwater around industrial areas (Fuge and Johnson, 2015). In precipitation, iodine concentrations range from 0.2 and 6 μg L^{-1} (Aldahan et al., 2009; Gilfedder et al., 2007a, 2008; Neal et al., 2007; Truesdale and Jones, 1996), and seem higher for oceanic than continental sites in Europe (e.g. Aldahan et al., 2009; Bowley, 2013). Iodine concentration in rain varied through a rainfall event, indicating progressive atmospheric washout (Duce et al., 1963; Fuge et al., 1987; Truesdale and Jones, 1996). In both rain and soluble fraction of aerosols, organo-iodine compounds account for over half of total iodine content, with a variable proportion of inorganic iodine (e.g. Baker, 2005; Campos et al., 1996; Gilfedder et al., 2007a, 2008; Lai et al., 2008; Truesdale and Jones, 1996). While Campos et al. (1996) and Truesdale and Jones (1996) recorded equal quantities of iodide (I^-) and iodate (IO_3^-) in rain, Gilfedder et al. (2007a) found higher proportions of iodide.

As iodine, atmospheric selenium is mainly originated from volatilisation from the marine environment (Wen and Carignan, 2007, 2009). Biogenic marine volatile methylated Se include dimethylselenide ($(CH_3)_2Se$), dimethyldiselenide ($(CH_3)_2Se_2$), methane selenol (CH_3SeH) and dimethyl selenyl sulphide ($(CH_3)_2SeS$), while dimethylselenide is dominant in biogenic continental emissions (Wen and Carignan, 2007, 2009). As expected by analogy with sulphur chemistry and investigated using quantum chemistry calculations, the reaction of methylated Se with radical hydroxyl (OH) produces dimethylselenoxide ($(CH_3)_2SeO$), which can be oxidized successively to elemental Se and selenium oxide (SeO) and then to water-soluble SeO_2 and selenous (H_2SeO_3) and selenic (H_2SeO_4) acids (Monahan-Pendergast et al. 2008; Wang and Tang, 2011). Atmospheric inorganic volatile selenium forms, elemental Se and SeO_2, also derive from volcanic and anthropogenic emissions (Wen and Carignan, 2007). Industrial sources include metallurgical industry, coal combustion, refuse incineration (Amouroux et al., 2001; Blazina et al., 2017; Mosher and Duce, 1987; Yudovich and Ketris, 2006). Long distance transport of atmospheric Se is expected after conversion of volatile to

particulate forms in which Se may occur in elemental, selenite (SeO_3^{2-}) and selenate (SeO_4^{2-}) species. Several studies have also investigated Se concentrations in precipitation (Blazina et al., 2017; Cutter and Church, 1986; De Gregori et al., 2002; Di Tullo, 2015; Ham and Tamiya, 2006; Lawson and Mason, 2001; Lidman et al., 2011; Pan and Wang, 2015; Sakata et al., 2006; Suess et al., 2019; Suzuki et al., 1981; Wang and Gao, 2001). Reported values, from 20 to 2,830 ng L^{-1}, vary in a wider range compared to iodine. Regarding speciation, inorganic selenium, in the forms of selenite and selenate, is essentially detected in waters including rainwaters. In precipitation in Europe, Robberecht et al. (1983), Floor et al. (2011) and Suess et al. (2019) reported that selenate was the major species (>65%). On the other hand, selenite was the most present (>50%) in rain in Tokyo (Suzuki et al., 1981), in the western Atlantic (Cutter and Church, 1986) and in Helsinki (Alfthan et al., 1995).

Unlike iodine and selenium, literature reporting levels of stable caesium in the atmosphere or in rainwaters is very limited. On the other hand, the ^{137}Cs radiocaesium was measured in rainwaters following the Fukushima and Chernobyl accidents, showing that its deposition is correlated with precipitation amount (e.g. Hötzl et al., 1989). Hence, the study of stable caesium as a proxy of radiocaesium allows to better predict the fate of released radiocaesium. In precipitation, the volume-weighted mean concentration of caesium in rain collected during two months in Lennox Mountain (Massachusetts) was 7.5 ng L^{-1} (Dasch and Wolff, 1989). Caesium has only one oxidation state (+1), and is present in waters as Cs^+ soluble cation which is not volatilized but can form insoluble complexes with suspended matter (Agency for Toxic Substances and Disease Registry, 2004). Atmospheric caesium is thus expected to exist mainly as particulate forms either oxides or sorbed onto aerosols in windblown seasprays and soil dust.

The Part I. of our work describes the spatial distribution and seasonal variations of iodine (^{127}I), selenium (^{78}Se) and caesium (^{133}Cs) atmospheric depositions at the level of France.

Twenty-seven forest sites, representative of five climates (i.e. oceanic, Mediterranean, transition, continental, mountainous), were monitored monthly in order to quantify I, Se and Cs concentrations and fluxes in rainfall (i.e. total precipitation including rain, snow, hail and dry deposition accumulated on the collectors). Iodine and selenium speciation in rainfall was also investigated. The aim of this Part I. is both to contribute to comprehensive data set of atmospheric depositions for these trace elements and to provide the basis to evaluate their interactions with tree canopy that will be the objective of the Part II. companion paper Roulier et al., 2020.

2. Materials and methods

2.1. Study sites

The 27 study sites are part of the French RENECOFOR network (the National Network for the long term Monitoring of Forest Ecosystems), managed by the ONF (National Forest Board) (www.onf.fr/renecofor) as part of the Integrated Co-operative Programme on Assessment and Monitoring of Air Pollution Effects on Forests (ICP Forests Level II) under the UNECE Air Convention (http://icp-forests.net/). All study sites are in forested areas, and in most cases are distant from cities or industrial emission sources (Ulrich et al., 1998). These sites are equipped with weather stations to sample rainfall (Figure 1). They are distributed throughout the French territory whose climate is temperate due to its middle latitude and the dominance of winds from Atlantic. The study sites are grouped in five main types of climates (oceanic, transition, continental, mountainous and Mediterranean) according to the temperatures, precipitation, latitude and altitude of the regions, as well as their proximity to the seas (Mediterranean Sea or English Channel) or the Atlantic Ocean, and their localisation compared to the three main mountain ranges (Pyrenees, Massif Central, Alps) (www.meteofrance.fr/climat-passe-et-futur/climat-en-france/le-climat-en-metropole) (SI

Table S1). In the rest of paper, the Mediterranean site (PL20) localized in Corsica is included in the Oceanic climate group.

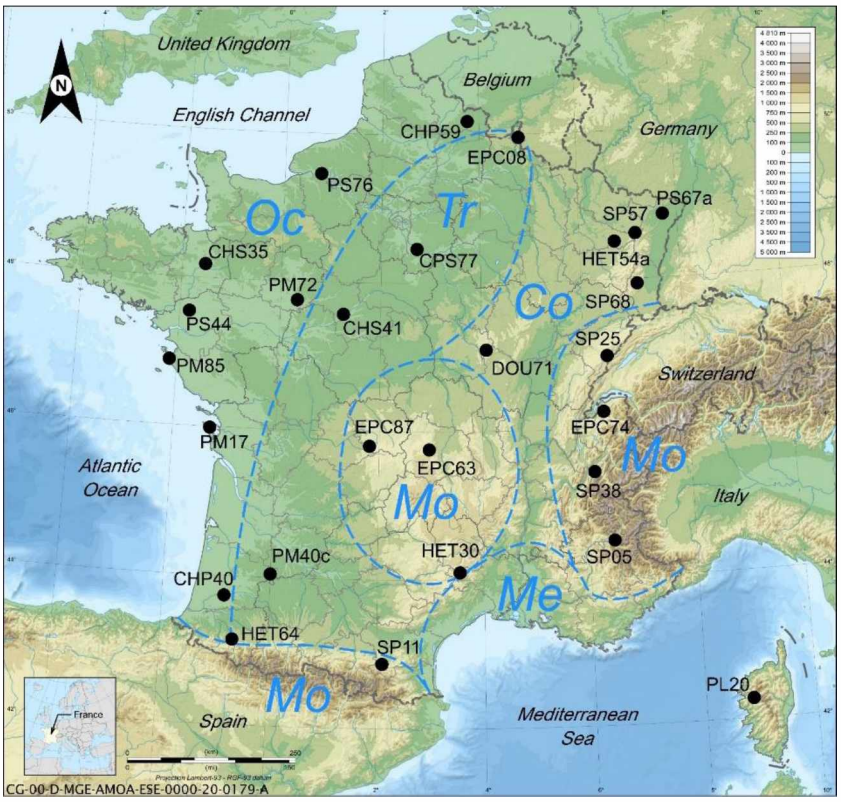

Figure 1. French climates and studied sites in the French RENECOFOR network (n = 27). Oc: Oceanic; Tr: Transition; Co: Continental; Mo: Mountainous; Me: Mediterranean. Base map: Eric Gaba (https://commons.wikimedia.org/w/index.php?curid=4899458).

2.2. Sampling procedure

Sampling procedure, detailed in Roulier et al. (2019), was based on the ICP Forests manual part XIV (Clarke et al., 2016). Briefly, rainfall was collected in bulk collectors (including dry deposition) once a week from September 2016 to September 2017 in open field areas while the precipitation amount was measured in a separate reference rain gauge (SPIEA 1650-01 model, graduated up to 100 mm). In order to avoid contamination of the samples with solid particles, the rims of the collectors were 1.0-1.5 m above ground level. The weekly samples were shipped to the laboratory in refrigerated tanks. Analyses were performed every 28 days on composite samples made from 4 weekly samples that were pooled in proportion to

their volume. Hence, a total of 13 composite samples was analyzed per site. The monthly basis composites were filtered at 0.45 µm with cellulose nitrate membrane filters, but were not acidified to prevent I losses through volatilization, and then stored in the dark at 4 °C until analysis. Hereafter, the four seasons were defined as follows: September 2016 to November 2016 and September 2017 (Autumn; n = 4/site), December 2016 to February 2017 (Winter; n = 3/site), March 2017 to May 2017 (Spring; n = 3/site), and June 2017 to August 2017 (Summer; n = 3/site).

2.3. Chemical analysis

2.3.1. Physicochemical properties of rainfall

The main physicochemical properties of the rainwater (i.e. pH, dissolved organic carbon and concentrations of major elements) were determined by the RENECOFOR network, following the ICP Forests manual part XIV (Clarke et al., 2016). The methods used and the limits of quantification are listed in SI Table S2. Briefly, most cations (Na, Mg, Ca, K) were analyzed by ICP-AES, anions (Cl^-, SO_4^{2-}, NO_3^-) by ionic chromatography, NH_4^+ by continuous flow UV-VIS-spectrophotometry, and dissolved organic carbon (DOC) with an elemental analyzer. Quality control was insured according to the ICP Forests manual part XVI (König et al., 2016). Samples were systematically re-analyzed in case the first results did not fulfill validation tests (ion balance, measured conductivity vs calculated from ion concentrations, Na/Cl ratio, total N vs sum of $N\text{-}NH_4$ and $N\text{-}NO_3$); in addition, the laboratory itself had successfully passed the international ring tests organized every two years in 2015 and 2017.

2.3.2. Analysis of iodine, selenium and caesium

The instrumental operating conditions for ICP-MS are summarized in SI Table S3. The quantification limits for total and speciation measurements were determined according to IUPAC recommendations as 10 × standard deviation of blanks divided by calibration slope.

Total soluble elemental concentrations were measured by inductively coupled plasma mass spectrometry (ICP-MS) (Agilent 7500ce for iodine and caesium, Agilent 7900 for selenium, Agilent Technologies, Japan). External calibrations in ultrapure water were prepared daily from individual I, Se and Cs single element standard 1 g L^{-1} (SCP Science). Quantification limits were 0.04 µg L^{-1}, 0.6 and 2 ng L^{-1} for total iodine (^{127}I), caesium (^{133}Cs) and selenium (^{78}Se), respectively. Typical analytical precision was lower than 5% (Relative Standard Deviation (RSD)).

An Agilent 1200 series HPLC pump was coupled to ICP-MS (Agilent 7900) for speciation analyses of iodine (iodide I^- and iodate IO_3^-) and selenium (selenite SeO_3^{2-} and selenate SeO_4^{2-}). Chromatographic separation was carried out on an anion exchange stationary phase (Agilent G3154-65001 column and G3154-65002 guard column, Agilent Technologies, Japan) with 20 mmol L^{-1} ammonium nitrate (≥ 99.5%, Sigma-Aldrich) as the mobile phase at pH 8.5 adjusted with ammonia (NH_4OH solution ≥ 25%, Fluka) delivered at 1 mL min^{-1} flow rate. Low percentage (2.5% v/v) of methanol (≥ 99.9%, Sigma-Aldrich) was added in the mobile phase to improve sensitivity. The sample injection volume was of 100 µL. Quantification was based on the standard addition method using daily diluted solutions of certified standards of 1 g L^{-1} iodide from Sigma-Aldrich and, 1 g L^{-1} iodate, 1 g L^{-1} Se as selenite and 0.1 g L^{-1} Se as selenate obtained from Spectracer. The quantification limits were 5 ng L^{-1} (I-IO_3^- and Se-SeO_4^{2-}) and 10 ng L^{-1} (I^- and Se-SeO_3^{2-}). Memory effects were checked by periodically running blanks between samples. The unidentified fraction (denoted "other" iodine and selenium: I_{other} and Se_{other}, respectively) was calculated as the difference between

total and inorganic species concentrations (i.e. $I_{other} = I - (I^- + IO_3^-)$ and $Se_{other} = Se - (SeO_3^{2-} + SeO_4^{2-})$). Since some samples were only available for analysis three months after sampling, we repeated an analysis on some samples three months after their first analysis to check the stability of the total concentrations and speciation during storage. Average gaps of 4 ± 4, 10 ± 5 and 2 ± 2% were found for I, I^- and IO_3^-, respectively. For selenium, the difference between the two analyses was 9 ± 6 and 8 ± 4% for Se and SeO_4^{2-}, respectively (SeO_3^{2-} was not detected in any re-analyzed samples). For Cs, the difference between analyses at 3-months intervals was on average of 7 ± 9%.

2.4. Calculation and data analysis

2.4.1. Calculation methods

For Se_{other} and following calculations, a value of one half the quantification limit, i.e. 5 ng L^{-1} as Se, was assigned to selenite concentration in samples that did not contain quantifiable level of this species.

To take into account the influence of sample volume on concentrations, the annual and seasonal volume-weighted mean (AVWM and SVWM, respectively) concentrations were calculated from elemental or species concentrations (c_i; µg L^{-1}) and the sample volume (V_i; mm) for the analysed time period as follow (Equation 1):

$$\text{AVWM or SVWM} = \frac{\Sigma_i (c_i \times V_i)}{\Sigma_i V_i} \qquad (1)$$

For SVWM concentrations, the four seasons were defined as follows: September 2016 to November 2016 and September 2017 (Autumn), December 2016 to February 2017 (Winter), March 2017 to May 2017 (Spring), and June 2017 to August 2017 (Summer).

The annual elemental flux (g ha^{-1} yr^{-1}) in rainfall (RF) was calculated as the sum of the monthly elemental concentrations in the water multiplied by the corresponding monthly water flux (provided by ONF-RENECOFOR).

2.4.2. Statistical analyses

Preliminary analyses were conducted to assess overall multivariate relationships between the different variables measured in our study. At first, a principal component analysis (PCA) was applied to the AVWM elemental concentrations from the 27 studied sites to evaluate preferential association between chemical elements in rainfalls. Second, relationships between pairs of variables were tested using Pearson's correlations to assess the relationship between pairs of quantitative variables and an analysis of variance (ANOVA) to assess relationships between quantitative and categorical variables. Prior to these analyses, the normality of the data was evaluated with a Shapiro-Wilk test. For variables that did not satisfy normality, a non-parametric approach was preferred with the Spearman's correlation and the Kruskal-Wallis to replace Pearson's correlations and ANOVA, respectively.

The relationships between each AVWM elemental concentrations and the explanatory variables (i.e. altitude and rainfall amount) were further investigated using ordinary least squares (OLS) multiple regression analyses. Statistical analyses and boxplot representations were performed with R programming environment (R Core Team, 2013, version 3.4.3).

3. Results and discussion

Detailed data for (a) annual water amount, annual pH mean, AVWM concentrations of DOC and major elements; (b) AVWM concentrations of total I, Se and Cs, and proportions of I and Se species; and (c) seasonal water amount and SVWM concentrations of total I, Se and Cs in rainfall for each site are available in SI Tables from S4 to S8.

3.1. Spatial and seasonal rainfall water fluxes and their physicochemical properties

Spatial differences in rainfall amounts were observed among sites; for the study period, annual rainfall ranged from 518 to 2,365 mm yr^{-1} (mean = 893 ± 391 mm yr^{-1}; SI Figure S1). The highest annual rainfall levels (760-1,270 mm yr^{-1}) were recorded in mid- and high-altitude mountains (altitude > 400 m), and were related to orographically induced rainfall. The southern HET30 site, located in the Cévennes Mountains (Figure 1) and characterised by strong convective rainfall (Vidal et al., 2010), had the highest annual rainfall (SI Figure S1; 2,365 mm yr^{-1}) as observed for previous years (mean annual rainfall between 1995 and 2007 = 2,400 mm yr^{-1}; Pascaud et al., 2016). Annual rainfall was the lowest (< 600 mm) in the western and northern areas influenced by a marine west-coast climate (SI Figure S1). A high variability in seasonal rainfall was also observed. Overall, monthly rainfall was higher at the end of autumn (November 2016) and beginning of spring (March 2017) and lower in winter (December 2016 and January 2017) and April 2017 (SI Figure S2). Rainfall pH values were mostly acidic, with mean annual values of 6.0 ± 0.5 (SI Table S4). Dissolved organic carbon (DOC) concentrations in rainfalls were very low (median = 0.50 mg L^{-1}) and therefore were not systematically detected.

3.2. Iodine, selenium, caesium and major elements in rainfall

3.2.1. Rainfall elemental concentrations

3.2.1.1. Spatial distribution

Sodium and chlorine were major elements in rainfall, with AVWM concentrations ranging from 0.20 to 3.94 mg L^{-1} (SI Table S5; median = 0.53 mg L^{-1}) and from 0.34 to 7.55 mg L^{-1} (median = 0.99 mg L^{-1}), respectively. Sea spray aerosols are the major contributors to Na and Cl in rainfall with molar Cl/Na ratio of seawater composition (i.e. 1.17; Bruland and Lohan, 2003). The slope of annual VWM Cl versus Na molar concentrations in rainfall equaled 1.23 ± 0.01 (SI Figure S3, R^2 = 0.99) and was thus comparable to the molar Cl/Na ratio in seawater; this is consistent with results of Blazina et al. (2017) obtained in England with a molar Cl/Na ratio in rainfall of 1.25. Hence, no significant depletion of Cl relative to Na seemed to occur, and rainwater composition indicated a marine influence as previously observed in France and Western Europe (Deboudt et al., 2004; Delalieux et al., 2006). Rains were also mostly composed of terrestrial ions with Ca (SI Table S5; median = 0.46 mg L^{-1}) mainly provided by dust from the Sahara Desert and/or the regional erosion of soils (Lequy et al., 2012), the anthropogenic components NO_3^- and NH_4^+, (median = 0.22 and 0.36 mg L^{-1}, respectively) from traffic, industry and agriculture sources (Bertrand et al., 2008; Pascaud et al., 2016), and SO_4^{2-} (median = 0.24 mg L^{-1}) from anthropogenic, volcanism and marine sources (Balestrini et al., 2007; Bertrand et al., 2008). AVWM I concentrations in rainfall varied between 0.82 and 2.70 µg L^{-1} (SI Table S6; median = 1.42 µg L^{-1}). These concentrations were similar to those reported by Neal et al. (2007) (1.41 µg L^{-1}) and Bowley (2013) (2.25 µg L^{-1}) in the U.K., Aldahan et al. (2009) (2.37-2.77 µg L^{-1}) in Sweden and Denmark, Lehto et al. (2012) (0.47-0.72 µg L^{-1}) in Finland, and Suess et al. (2019) (0.34-1.29 µg L^{-1}) in Switzerland and France. In our study, selenium and caesium concentrations in rainwater were much lower than those of iodine, ranging from few ng L^{-1} to tens of ng L^{-1}. AVWM Se concentrations ranged between 23 and

85 ng L^{-1} (SI Table S6; median = 44 ng L^{-1}). This is in the lowest range of Se concentrations reported in rainwater in Europe (40-1,600 ng L^{-1}) as reviewed by Conde and Sanz Alaejos (1997), in China (30-590 ng L^{-1}; Wang and Gao, 2001), and in Japan (100-1,400 ng L^{-1}; Ham and Tamiya, 2006). Comparable Se concentrations were reported in rain from Northern Sweden and Finland (50 and 120 ng L^{-1}, Lidman et al., 2011) and from rural and agricultural areas in Chile (40 and 130 ng L^{-1}; De Gregori et al., 2002). More recently, Blazina et al. (2017) reported rainfall Se concentrations in the U.K. ranging from 310 to 2,830 ng L^{-1}, and Suess et al. (2019) from 20 to 50 ng L^{-1} for two Swiss and French high-altitude sites. Very little is known about stable caesium concentrations in rainfall, since most studies on caesium in rain focused on ^{137}Cs release after the Chernobyl and Fukushima accidents. The values measured in this study, between 2 and 13 ng L^{-1} (median = 5 ng L^{-1}), are similar to those reported in Massachusetts precipitation (5-24 ng L^{-1}; Dasch and Wolff, 1987) and are thus in the lower range of stable caesium concentrations in fresh water, lakes and rivers (10-1,200 ng L^{-1}; Burger and Lichtscheidl, 2018).

In order to determine similarities between the chemical elements in rainfall, the principal component analysis (PCA) applied to the AVWM elemental concentrations for the 27 studied sites is shown Figure 2. The variables included concentrations of elements of interest (i.e. I, Se and Cs), concentrations of major elements (i.e. Na, Cl, Mg, Ca, K, SO_4^{2-}, NO_3^- and NH_4^+), DOC concentrations and annual rainfall amounts. The first three PC axes explained 76.8% of the total variance of data (Table 1), and only the first two axes are represented (Figure 2; 65.3% of the total variance). The first PC axis (44% of the total variance) suggested that both iodine and selenium were associated with elements of marine origin (Na, Cl, Mg, SO_4^{2-}) as well as with certain elements mainly of terrestrial origin (Ca, K, SO_4^{2-}) and with DOC of biogenic (e.g. marine environment, vegetation) and anthropogenic (e.g. fossil fuel combustion) sources. The second PC axis (21.3% of the total variance) highlighted association of anthropogenic

components (NH_4^+, NO_3^-) and Cs. The third PC axis associated selenium concentrations and rainfall amount (11.5% of the total variance).

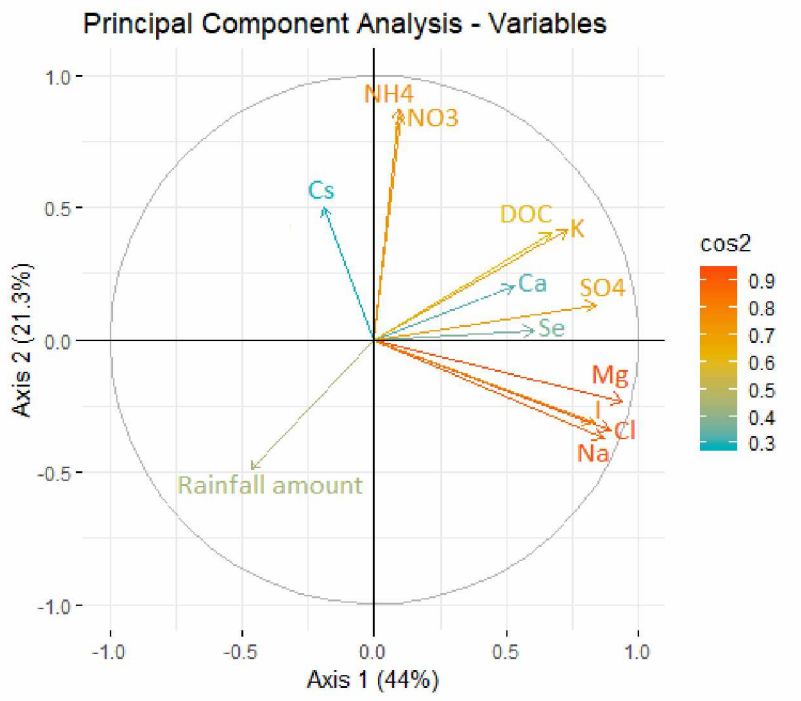

Figure 2. The correlation circle of the principal component analysis (PCA) showing the contribution of AVWM elemental concentrations in rain and annual rainfall amount on the first two PC axes. Representation of the variables on PC axis 1 and 2 is expressed in cos2.

Table 1. The contribution (loadings) of each AVWM elemental concentrations in rain and annual rainfall amount on the first three PC axes. The percentage of variance explained by each axis is given in parentheses. Bold indicates that the variable correlates well with the axis.

Axis (% of the total variance)	PC1 (44)	PC2 (21.3)	PC3 (11.5)
Rainfall amount (mm)	-0.461	-0.486	**0.628**
Na (mg L^{-1})	**0.870**	-0.373	-0.104
Cl (mg L^{-1})	**0.891**	-0.342	-0.111
Mg (mg L^{-1})	**0.939**	-0.230	-0.040
Ca (mg L^{-1})	**0.528**	0.203	0.031
K (mg L^{-1})	**0.732**	0.413	-0.231
SO_4^{2-} (mg L^{-1})	**0.840**	-0.133	0.249
NH_4^+ (mg L^{-1})	0.091	**0.873**	0.152
NO_3^- (mg L^{-1})	0.102	**0.843**	0.453
DOC (mg L^{-1})	**0.669**	0.406	-0.367
I (µg L^{-1})	**0.831**	-0.315	0.223
Se (ng L^{-1})	**0.604**	0.035	**0.732**
Cs (ng L^{-1})	-0.193	**0.501**	-0.091

The PCA clearly showed a high positive relationship between AVWM I, Na, Cl and Mg concentrations consistent with their common marine origin in the rains. Consequently, AVWM I concentrations were significantly higher under oceanic climate than for transition, continental and mountainous sites (Figure 3 (b); Kruskal-Wallis test, $p < 0.001$). Likewise, Aldahan et al. (2009) and Bowley (2013) determined higher iodine concentrations in rainfall from coastal areas compared to continental sites. In the current study, the PCA showed common patterns between selenium and both marine and terrestrial components consistent with the various sources of Se in atmosphere (i.e. natural marine and terrestrial sources + anthropogenic releases) resulting in no significant difference between AVWM Se concentrations in rains under oceanic, transition and continental climates (Figure 3 (c); Kruskal-Wallis test, $p < 0.05$). Unlike I and Se, AVWM Cs concentrations in rainfall were significantly higher for continental sites than for oceanic, transition and mountainous sites (Figure 3 (d); Kruskal-Wallis test, $p < 0.05$). Caesium concentrations in rainfall might have a terrestrial origin, such as atmospheric dusts derived from wind erosion of the Earth's surface which contains Cs. The association of Cs with NH_4^+ and NO_3^- (Table 1 and Figure 2) supports this hypothesis since the latter two anthropogenic components are used in agriculture and when soils are tilled, suspended soil particles are released into the atmosphere.

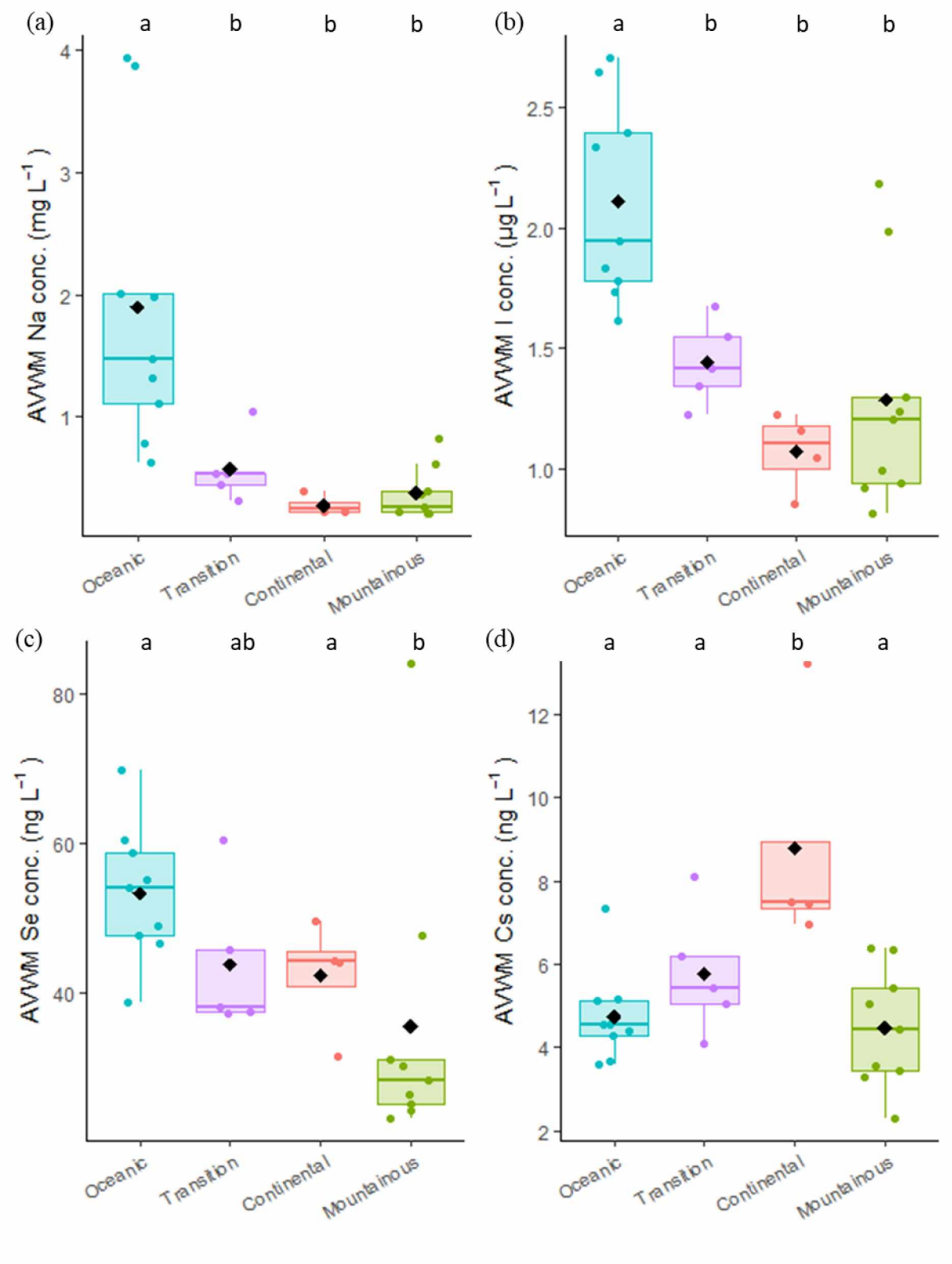

Figure 3. Distribution of AVWM concentrations of (a) sodium, (b) iodine, (c) selenium and (d) caesium in rains across the four climates. The Mediterranean site (PL20) is included in the Oceanic climate group. Distributions are represented by boxplots based on the five-number summary, that is: minimum, first quartile, median, third quartile and maximum. Black diamonds indicate mean value. Climates accompanied by a different letter are significantly different from each other (pairwise Wilcoxon test, with Holm adjustment for *p*-values).

Iodine and selenium concentrations were also influenced by orographically induced precipitation as indicated by the results of a multiple regression analysis (Table 2). Indeed, AVWM concentrations of both I and Se in rainfall decreased with increasing altitude (Table 2; $p < 0.05$). On the contrary, there was no link between AVWM Na and Cs concentrations in rainfall and site altitude (Table 2; $p > 0.05$). These results are consistent with previous studies suggesting that iodine concentrations in rainfall are also influenced by an orographically induced removal effect (Aldahan et al., 2009; Gilfedder et al., 2007b; Reithmeier et al., 2006). Indeed, Gilfedder et al. (2007b) study on orographically induced precipitation demonstrated that iodine concentrations in rainfall significantly decreased with altitude.

Table 1. Statistical analyses for AVWM Na, I, Se and Cs concentrations in rain. Summary of *p*-values obtained through multiple regression analyses.

Candidate explanatory variables	**Sodium**	**Iodine**	**Selenium**	**Caesium**
Altitude	0. 0649	< 0.05	< 0.05	0.8380
Rainfall amount	0.6952	0.2043	< 0.05	0.8180

3.2.1.2. Seasonal variability

Considering all sites and months, monthly Na, I, Se and Cs concentrations in rainfall ranged from 0.06-11.62 mg L^{-1}, 0.30-4.73 µg L^{-1}, 8-472 and 1-32 ng L^{-1}, respectively. Sodium and caesium concentrations varied considerably throughout the year within the same site (for the 27 sites average factor of 15 and 8, respectively) more markedly than those of I and Se (average factor of 4 and 5, respectively). In past research on rainfall chemistry, the relationship between elemental concentrations and rainfall amount has been mentioned many times and attributed mainly to the washing out of elements during precipitation and/or to the rainfall dilution effect (e.g. Blazina et al., 2017; Suess et al., 2019; Suzuki et al., 1981; Xu et al., 2016). In our study, considering all sites and months there was no relationship between monthly Na, I, Se or Cs concentrations and monthly rainfall amounts (SI Figure S4).

The changes in SVWM Na, I, Se and Cs concentrations in rainfall in four seasons according to climates are presented Figure 4. Under oceanic and transition climates, SVWM Na concentrations were significantly higher in winter and spring than in summer and autumn (Figure 4 (a); Kruskal-Wallis test, $p < 0.05$). This finding is in accordance with previous studies indicating that higher sodium concentrations in winter may be due to the greater amount of maritime air recorded during this season, and western air masses from the Atlantic Ocean in France are more frequent at this period of the year (Calvo et al., 2012; Thimonier et al., 2008). However, for continental and mountainous sites, sodium concentrations were not significantly different from one season to another (Kruskal-Wallis test, $p > 0.05$). Unlike sodium, SVWM I concentrations were generally significantly higher in summer and autumn than in winter and spring for all climates (Figure 4 (b); Kruskal-Wallis test, $p < 0.05$). For other European sites, Campos et al. (1996) (England), Gilfedder et al. (2007a) (Germany and Switzerland), Aldahan et al. (2009) (Sweden and Denmark) and Suess et al. (2019) (Switzerland) also observed an increase in iodine concentrations over the summer months. Whereas for some English sites, Truesdale and Jones (1996) and Baker et al. (2001) noted no relationship between rainfall I concentrations and season. Baker et al. (2001) explained this lack of seasonal trend by the important influence of wind speed changes on sea spray inputs. Moreover, previous works have shown that terrestrial areas receive higher amounts of moisture derived from the continent in summer, spring and autumn than they do in winter (Calvo et al., 2012; Pio et al., 2007; Pupier et al., 2016; Suess et al., 2019; Thimonier et al., 2008). Consequently, higher concentrations of I in the warmest months (summer-autumn) could be due to a higher contribution of continental sources (e.g. volatilization of I, evapotranspiration through soil and vegetation, wind-borne soil dust) during these warmest seasons. On the other hand, in the current study, SVWM Se concentrations were higher in summer only for mountainous climates (Figure 4 (c); Kruskal-Wallis test, $p < 0.05$). In our study, no clear seasonality was observed for Cs with SVWM

concentrations showing similar trend as annual ones with higher seasonal values under continental climate in all seasons (Figure 4 (d)).

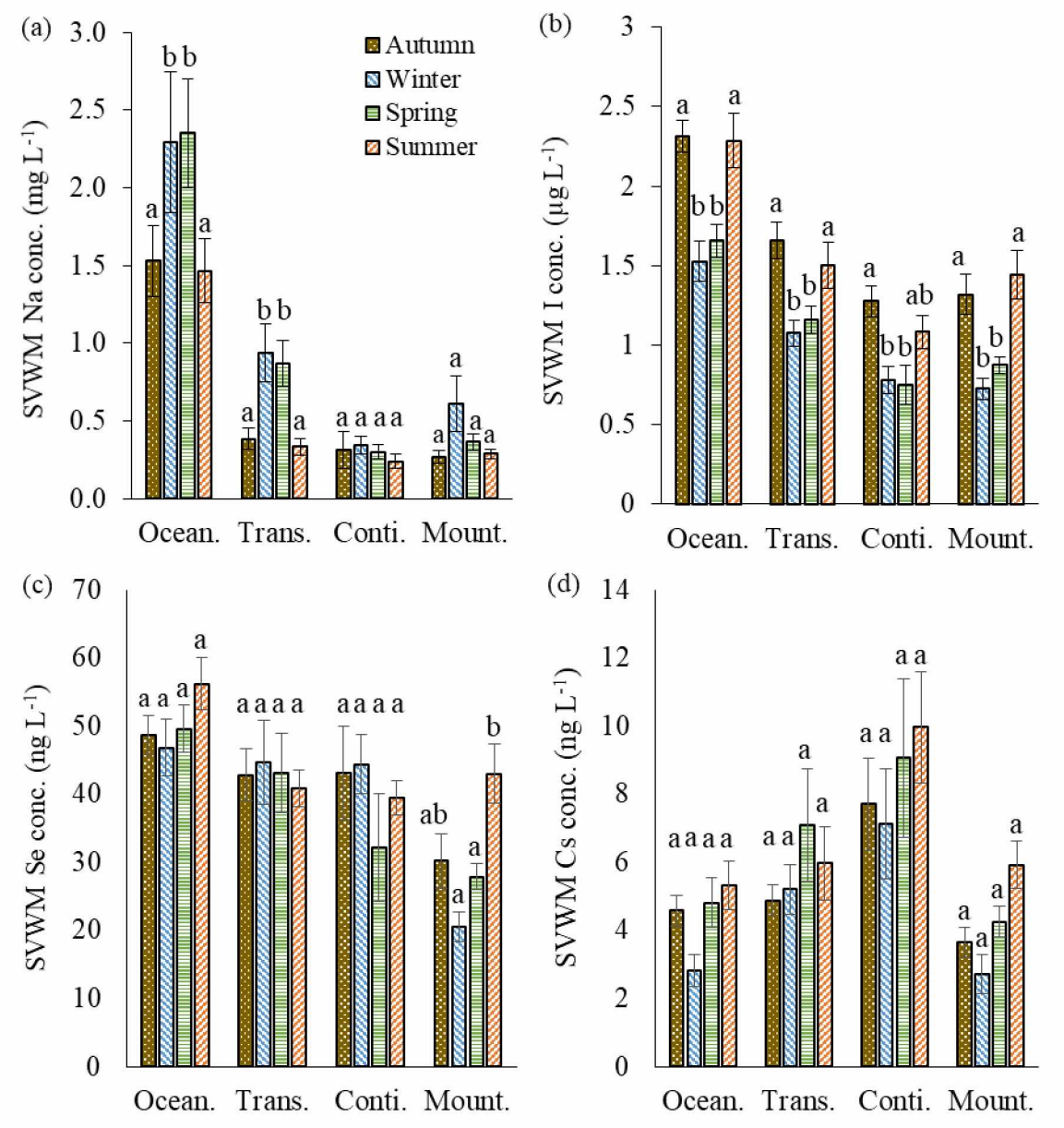

Figure 4. Seasonal volume weighted mean (SVWM) concentrations of (a) sodium, (b) iodine, (c) selenium and (d) caesium in rainfall according to climate (n = 26 sites, the mountainous HET30 site was excluded due to its exceptionally high water amount). The Mediterranean site (PL20) is included in the Oceanic climate group. Error bars correspond to standard errors. Ocean. = Oceanic, Trans. = Transition, Conti. = Continental and Mount. = Mountainous. The four seasons were defined as follows: September 2016 to November 2016 and September 2017 (Autumn; n = 4/site), December 2016 to February 2017 (Winter; n = 3/site), March 2017 to May 2017 (Spring; n = 3/site), and June 2017 to August 2017 (Summer; n = 3/site). For each climate, seasons accompanied by a different letter are significantly different from each other (Post hoc Dunn test after significant Kruskal-Wallis test).

3.2.2. Rainfall elemental fluxes

Since rainfall amounts and elemental concentrations varied significantly from month to month, as expected their rainfall fluxes showed significant monthly variations within the same site. Considering all sites and months, ranges for monthly Na, I, Se and Cs RF were 0.001-0.712 g m^{-2} $month^{-1}$, 0.01-1.29 mg m^{-2} $month^{-1}$, 0.2-77.4 and 0.04-3.59 µg m^{-2} $month^{-1}$, respectively. Ranges of annual rainfall I, Se and Cs fluxes were: 7.6-51.8, 0.25-2.01 and 0.02-0.12 g ha^{-1} yr^{-1}, respectively (SI Figures S5). The sites HET30, HET64 and PL20 had the highest I and Se rainfall fluxes (> 27 and > 0.70 g ha^{-1} yr^{-1}) due to both the highest annual rainfall amounts (> 1,000 mm yr^{-1}) and their proximity to coasts (< 80 km), which resulted in higher AVWM I and Se concentrations (I: 2.2, 2.0 and 2.7 µg L^{-1}, Se: 85, 51 and 70 ng L^{-1}; for HET30, HET64 and PL20, respectively). Excluding these three sites, there was very little variation among rainfall I and Se fluxes according to climate (SI Figure S6; mean RF(I) = 13.7 ± 3.3, 11.9 ± 3.0, 8.8 ± 1.4 and 11.8 ± 1.7 g ha^{-1} yr^{-1}; mean RF(Se) = 0.35 ± 0.08, 0.36 ± 0.13, 0.35 ± 0.07 and 0.33 ± 0.06; for oceanic, transition, continental and mountainous climates, respectively). Such values are in the same order of magnitude as those previously reported in Sweden and Denmark (3.4-15 g ha^{-1} yr^{-1} (2000-2006 period); Aldahan et al., 2009) and, in North-Eastern France (15.4 ± 1.7 g ha^{-1} yr^{-1} (2014-2016 period); Roulier et al., 2018). Aldahan et al. (2009) also observed higher values at sites near coasts compared to inland ones. Annual Se inputs associated to rainfall were comparable to those previously reported in the North-East of France (1.11 g ha^{-1} yr^{-1}; Di Tullo, 2015), in Northern Finland and Sweden (0.43 to 0.49 g ha^{-1} yr^{-1}; Lidman et al., 2011), in China (0.15 to 0.3 g ha^{-1} yr^{-1}; Wang and Gao, 2001) and in the western Atlantic (0.45-1.5 g ha^{-1} yr^{-1}; Cutter and Church, 1986). Concerning Cs, highest rainfall fluxes of 0.12 g ha^{-1} yr^{-1} were quantified at two sites (HET30 and SP68) due to highest annual rainfall amount and highest AVWM Cs concentration, respectively. With the exception of these two sites, Cs rainfall fluxes under oceanic climate (0.033 ± 0.008 g ha^{-1} yr^{-1}) were

slightly lower compared to other climates (0.05 ± 0.02, 0.06 ± 0.02 and 0.05 ± 0.02 g ha^{-1} yr^{-1} for transition, continental and mountainous climates, respectively).

3.2.3. Iodine and Selenium species in rainfall

3.2.3.1. Iodine species

The annual contributions of I^-, IO_3^- and "other" iodine compound(s) in rain ranged from 8-44, 16-37 and 39-66%, respectively (Figure 5 (a); means = 25.55, 24.85 and 49.60%, respectively). Therefore, over the year, the rains contained on average equal proportions of inorganic and "other" iodine compounds. In Central Europe, Gilfedder et al. (2007a) also observed that iodine was mostly organically bound (about 56%) and that iodide was more abundant than iodate (about 27 and 10%, respectively).

In the current study, iodide proportions were significantly higher in rains under continental and mountainous climates than under oceanic climate (Figure 6 (a); Kruskal-Wallis test, $p < 0.001$). On the other hand, iodate proportions were significantly higher in rains under oceanic and transition climates than under continental and mountainous climates (Figure 6 (b); Kruskal-Wallis test, $p < 0.001$). These results are in line with some previous findings indicating that the share of IO_3^- is higher in marine-derived rainfall than in continental rainfall (e.g. Gilfedder et al., 2007a; Gilfedder et al., 2008). Gilfedder et al. (2007a) found that soluble organically bound iodine (calculated as total iodine minus inorganic iodine species) was the dominant fraction in all rain samples collected in Australia, New Zealand, Patagonia, Germany, Ireland and Switzerland, generally accounting for 50-80% of total iodine. They hypothesized that soluble organically bound iodine would be formed by a reaction between organic matter derived from the ocean's surface layer and HOI and/or I_2 produced by the oxidation of I^-, and/or the reduction of IO_3^-. In our study, no correlation between "other" iodine fraction and DOC concentrations was found (results not shown). This lack of correlation could be explained by

the various sources of DOC in rains that can be both biogenic and anthropogenic. However, two unknown iodine containing peaks were detected in rainwater samples in addition to inorganic compounds (SI Figure S7 (a)). With similar anionic chromatographic analysis, Gilfedder et al. (2008) also detected unidentified iodine-containing compounds, likely anionic organic iodine species, in both aerosols and rainfall, suggesting that these species were transferred from aerosols to rainwater.

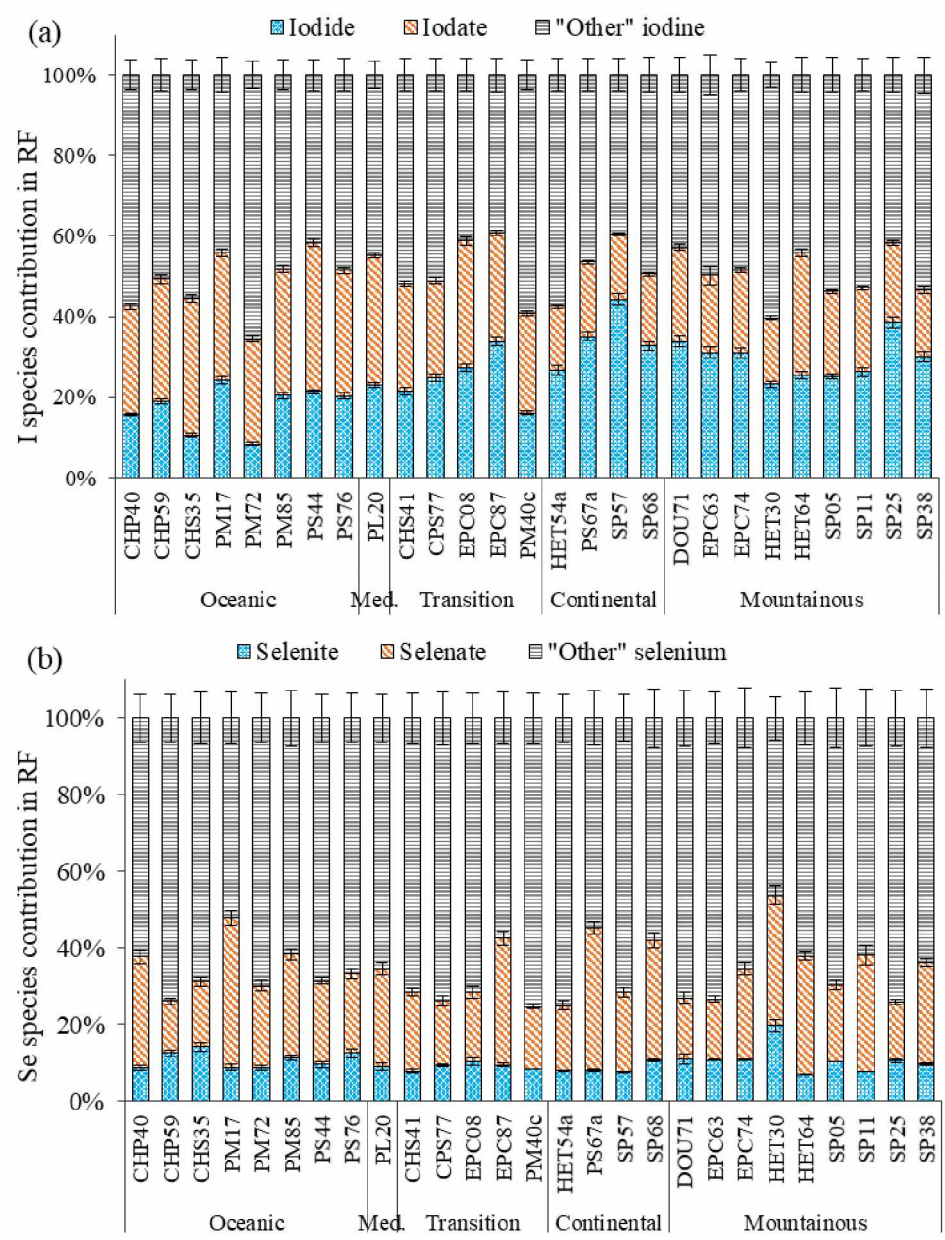

Figure 5. Annual proportions of (a) iodide, iodate and "other" iodine and (b) selenite, selenate and "other" selenium in rainfall at the study sites classified according to climate (n = 27 sites). Med.: Mediterranean. Error bars show the standard errors.

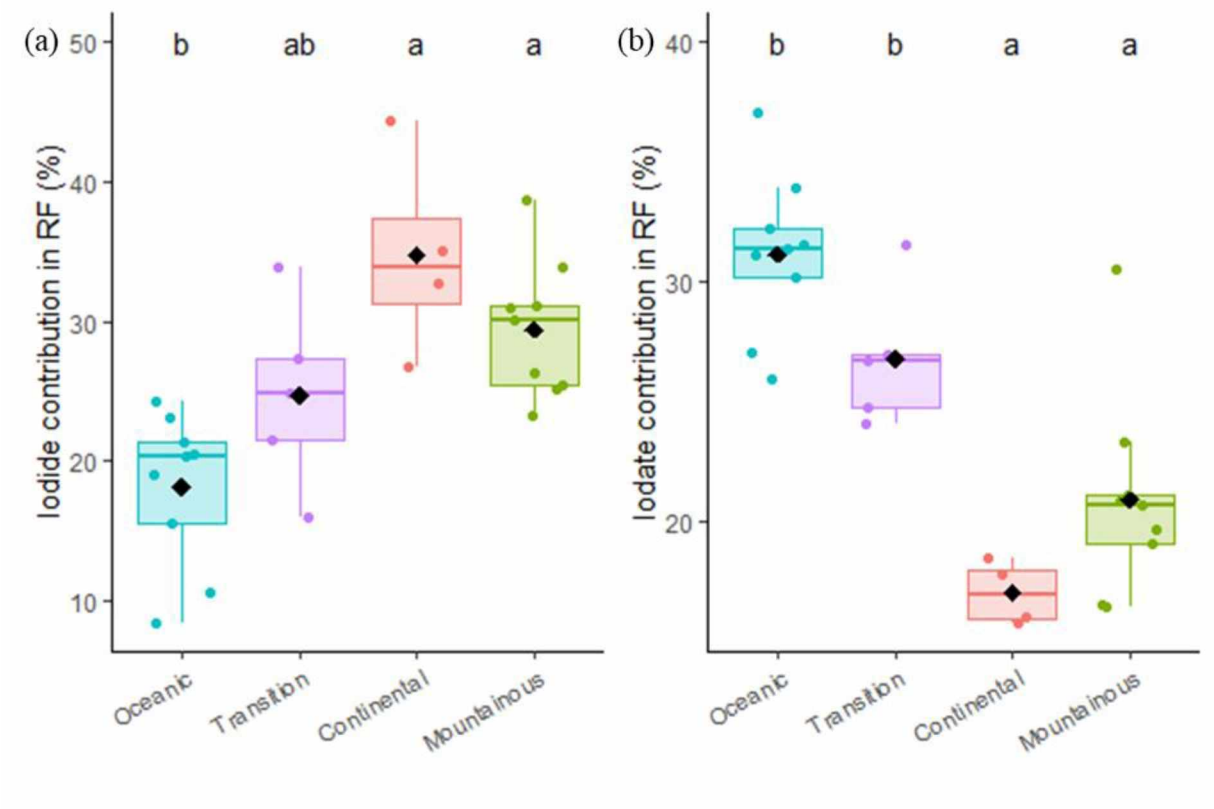

Figure 6. Distribution of (a) iodide and (b) iodate proportions in rains across the four climates. The Mediterranean site (PL20) is included in the Oceanic climate group. Distributions are represented by boxplots based on the five-number summary, that is: minimum, first quartile, median, third quartile and maximum. Black diamonds indicate mean value. Climates accompanied by a different letter are significantly different from each other (pairwise Wilcoxon test, with Holm adjustment for p-values).

The contributions of I^- and IO_3^- in rainfall showed an important monthly variability within the same site whatever the climate conditions. Although iodine speciation could depend on rainfall pH, no link was found between the variability of iodine species concentrations (or proportions) and rainfall pH (results not shown). Whereas iodide showed no clear seasonal trend (SI Figure S8 (b); Kruskal-Wallis test, $p > 0.05$ except for mountainous climate with $p < 0.001$), iodate proportions significantly increased during winter (SI Figure S8 (a); Kruskal-Wallis test, $p < 0.001$ for all climates), especially under oceanic and transition climates. This result is consistent with expected contribution of moisture from marine sources (contributing to a higher IO_3^- proportion) which is more important in winter than during warmer months, resulting in the

decrease of iodate fraction in summer. The lack of seasonal trend for iodide might be explained by its oxidation and subsequent reaction with atmospheric compounds. Indeed, iodide oxidized to I_2 or HOI is likely to react with atmospheric organic compounds derived from the oceanic surface micro layer or from a terrestrial source (Gilfedder et al., 2007a). Contrary to our results, for a site in southern Germany, Gilfedder et al. (2007a) found no strong seasonal patterns in inorganic iodine speciation. However, in contrast, organically bound iodine concentrations and their percentages were higher during summer months than in winter. In our study, the "other" iodine compounds fraction showed no clear monthly pattern (SI Figure S8 (c); Kruskal-Wallis test, $p > 0.05$ for all climates). We detected two unknown iodine containing peaks but this unidentified fraction could correspond to a mixture of various iodine compounds due to both (1) organic iodine directly derived from marine and continental sources and (2) reaction between iodine and atmospheric organic carbon compounds (gaseous or particulate matter).

3.2.3.2. Selenium species

An example of IC-ICP-MS chromatogram of inorganic selenium species in rainfall is shown in SI Figure S7 (b). Most of the rains had selenite concentrations below the limit of quantification and the value of 5 ng L^{-1} as Se (half of the quantification limit) was assigned to selenite concentration in these samples. In annual average, rainfall contained mostly "other" selenium compounds and inorganic selenium was clearly minor pool (range and mean = 7-20 and 10, 14-39 and 24, 46-75 and 66%, for SeO_3^{2-}, SeO_4^{2-} and Se_{other} respectively). Only the mountain site HET30 had equal levels of inorganic Se and other unidentified compounds. Suess et al. (2019) reported that selenium was mainly present as SeO_4^{2-} with average contributions of around 65-84% at high altitude Swiss and French sites. These authors also indicated that the presence of unidentified Se accounted for up to 60% of total Se. Higher proportions of selenate were reported for rainwater sampled in Antwerp (80%; Robberecht et al., 1983) and on the

Mount Etna volcano (67%; Floor et al., 2011). On the contrary, selenite was the major species detected in rains in Helsinki (60%; Alfthan et al., 1995), Tokyo (50-90%; Suzuki et al., 1981) and the western Atlantic (66% on average; Cutter and Church, 1986). In our study, for all sites, AVWM selenate concentrations were significantly positively correlated with those of Se (Figure 7, $R^2 = 0.65$; Spearman's correlation, $p < 0.001$), whereas no correlation was found with climate (Kruskal-Wallis test, $p > 0.05$). As for iodine species, the contributions of SeO_3^{2-} and SeO_4^{2-} in rainfall varied significantly from month to month within the same site whatever the climate (SI Figure S9), and no link with rainfall pH was found (results not shown). Selenium volatilization by microbial methylation (from marine and continent biospheres), and industrial activities contribute to the release of atmospheric Se into various organic and inorganic forms (e.g. Låg and Steiness, 1974; Suess et al., 2019; Vriens et al., 2014; Wen and Carignan, 2007). Spatial and temporal variations in selenium speciation in rainfall reflect thus the various atmospheric pathways, from emission to deposition, of these various emitted sources affected by oxidation reactions during atmospheric transport.

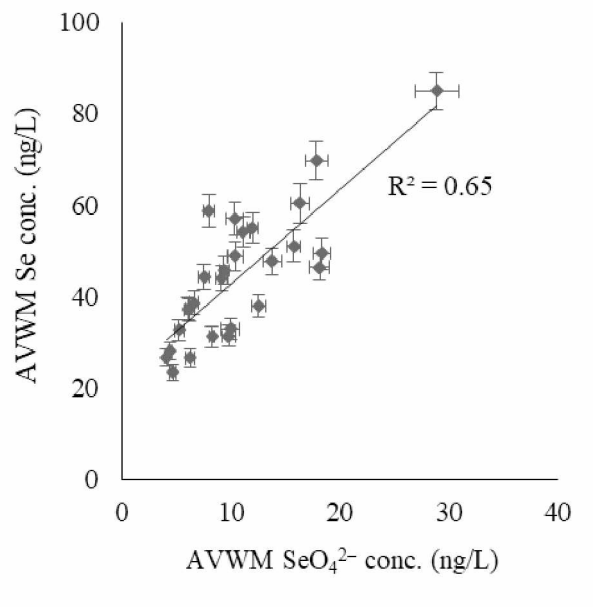

Figure 7. Relationships between AVWM total Se and selenate concentrations in rainfall. Error bars correspond to standard errors.

4. Conclusion

In this work, we analysed the spatial and seasonal variations of I, Se, Cs in rainfall in 27 forest sites all over France. The results of one year of monitoring indicated that annual volume weighted mean concentrations of iodine in rainfall were much higher than those of Se and Cs (factor ≈ 35 and 312, respectively), and significantly higher under oceanic climate than for transition, continental and mountainous sites which is consistent with a predominant atmospheric marine source. Spatial distribution of annual Se concentrations was not so clear probably due to the various sources of Se in atmosphere (natural marine and terrestrial sources + anthropogenic releases); while Cs concentration was significantly higher under continental climate. The association of Cs with agricultural anthropogenic NH_4^+ and NO_3^- elements supports a more terrestrial origin of this element in rainfall. Resulting annual rainfall fluxes of iodine and selenium were relatively homogeneous (12 ± 3 and 0.34 ± 0.08 g ha^{-1} yr^{-1}, respectively) with the exception of three sites with annual pluviometry above 1000 mm yr^{-1} that coincide with highest annual concentrations. Annual average rainfall deposition was composed in equal proportions of inorganic and unidentified I compounds, and mostly of unidentified Se compounds which proportion was higher than the one of inorganic selenium detected mainly as selenate. Qualitative and quantitative description of atmospheric deposits of stable selenium, iodine and caesium presented in this paper was the necessary first step to further investigate their interactions with tree canopies that will be presented in the Part II. of this paper.

Credit author statement

Roulier Marine: Conceptualization, Investigation, Validation, Formal analysis, Writing - original draft, Writing - review & editing; Maïté Bueno: Conceptualization, Investigation, Validation, Funding acquisition, Writing - review & editing, Supervision; Frédéric Coppin: Conceptualization, Validation, Funding acquisition, Writing - review & editing, Supervision; Manuel Nicolas: Resources, Writing - review & editing; Yves Thiry: Conceptualization, Funding acquisition, Writing - review & editing; François Rigal: Formal analysis, Validation, Writing - review & editing; Isabelle Le Hécho: Conceptualization, Writing - review & editing, Supervision; Florence Pannier: Conceptualization, Writing - review & editing, Supervision.

Declaration of competing interest

The authors declare that they have no known competing financial interests or personal relationships that could have appeared to influence the work reported in this paper.

Acknowledgments

We thank the technical staff of RENECOFOR-ONF for providing samples for this study as well as datasets other than those for iodine, selenium and caesium. This work was financed by the Région Nouvelle Aquitaine and the Agence Nationale de la Recherche with funds allocated in the 'Investissements d'Avenir' framework program under the reference ANR11-RSNR-0002. The authors thank Vicki Moore for English language assistance. The authors would like to thank Guy Pernot from the computer graphics Unit of Andra for his help in maps edition.

Appendix A. Supplementary data

Supplementary data to this article can be found online at https://doi.org/10.1016/j.chemosphere.2020.128971.

References

Agency for Toxic Substances and Disease Registry, 2004. US Department of Health and Human Services. Toxicological Profile for Cesium 306.

Aldahan, A., Persson, S., Possnert, G., Hou, X.L., 2009. Distribution of ^{127}I and ^{129}I in precipitation at high European latitudes. Geophysical Research Letters 36. https://doi.org/10.1029/2009GL037363

Alfthan, G., Wang, D., Aro, A., Soveri, J., 1995. The Geochemistry of Selenium in Groundwaters in Finland. Science of the Total Environment 162, 93–103. https://doi.org/10.1016/0048-9697(95)04436-5

Amouroux, D., Liss, P.S., Tessier, E., Hamren-Larsson, M., Donard, O.F., 2001. Role of oceans as biogenic sources of selenium. Earth and Planetary Science Letters 189, 277–283. https://doi.org/10.1016/S0012-821X(01)00370-3

Baker, A.R., Tunnicliffe, C., Jickells, T.D., 2001. Iodine speciation and deposition fluxes from the marine atmosphere. Journal of Geophysical Research: Atmospheres 106, 28743–28749. https://doi.org/10.1029/2000JD000004

Baker, A.R., 2005. Marine Aerosol Iodine Chemistry: The Importance of Soluble Organic Iodine. Environmental Chemistry 2, 295-98. https://doi.org/10.1071/EN05070

Balestrini, R., Arisci, S., Brizzio, M.C., Mosello, R., Rogora, M., Tagliaferri, A., 2007. Dry deposition of particles and canopy exchange: Comparison of wet, bulk and throughfall deposition at five forest sites in Italy. Atmospheric Environment 41, 745–756. https://doi.org/10.1016/j.atmosenv.2006.09.002

Bertrand, G., Celle-Jeanton, H., Laj, P., Rangognio, J., Chazot, G., 2008. Rainfall chemistry: long range transport versus below cloud scavenging. A two-year study at an inland station (Opme, France). Journal of Atmospheric Chemistry 60, 253–271. https://doi.org/10.1007/s10874-009-9120-y

Blazina, T., Läderach, A., Jones, G.D., Sodemann, H., Wernli, H., Kirchner, J.W., Winkel, L.H.E., 2017. Marine Primary Productivity as a Potential Indirect Source of Selenium and Other Trace Elements in Atmospheric Deposition. Environmental Science & Technology 51, 108–118. https://doi.org/10.1021/acs.est.6b03063

Bowley, H.E., 2013. Iodine dynamics in the terrestrial environment. PhD Thesis. University of Nottingham.

Bruland, K.W., Lohan, M.C., 2003. Controls of Trace Metals in Seawater, in: Treatise on Geochemistry, edited by H. Elderfield, 625 pp., Elsevier, Atlanta, USA

Burger, A., Lichtscheidl, I., 2018. Stable and radioactive cesium: A review about distribution in the environment, uptake and translocation in plants, plant reactions and plants' potential for bioremediation. Science of the Total Environment 618, 1459–1485. https://doi.org/10.1016/j.scitotenv.2017.09.298

Calvo, A.I., Pont, V., Olmo, F.J., Castro, A., Alados-Arboledas, L., Vicente, A.M., Fernandez-Raga, M., Fraile, R., 2012. Air Masses and Weather Types: A Useful Tool for Characterizing Precipitation Chemistry and Wet Deposition. Aerosol and Air Quality Research 12, 856–878. https://doi.org/10.4209/aaqr.2012.03.0068

Campos, M., Nightingale, P.D., Jickells, T.D., 1996. A comparison of methyl iodide emissions from seawater and wet depositional fluxes of iodine over the southern North Sea. Tellus Series B Chemical and Physical Meteorology 48, 106–114. https://doi.org/10.1034/j.1600-0889.1996.00010.x

Clarke, N., Žlindra, D., Ulrich, E., Mosello, R., Derome, J., Derome, K., König, N., Lövblad, G., Draaijers, G.P.J., Hansen, K., Thimonier, A., Waldner, P., 2016. Part XIV: Sampling and Analysis of Deposition. In: UNECE ICP Forests Programme Co-ordinating Centre (ed.): Manual on methods and criteria for harmonized sampling, assessment,

monitoring and analysis of the effects of air pollution on forests. Thünen Institute of Forest Ecosystems, Eberswalde, Germany, 32 p. + Annex.
Conde, J.E., Sanz Alaejos, M., 1997. Selenium Concentrations in Natural and Environmental Waters. Chemical Reviews 97, 1979–2004. https://doi.org/10.1021/cr960100g
Cutter, G.A., Church, T.M., 1986. Selenium in western Atlantic precipitation. Nature 322, 720. https://doi.org/10.1038/322720a0
Dasch, J.M., Wolff, G.T., 1989. Trace Inorganic Species in Precipitation and Their Potential Use in Source Apportionment Studies. Water, Air, & Soil Pollution 43, 401-12. https://doi.org/10.1007/BF00279205
De Gregori, I., Lobos, M.G., Pinochet, H., 2002. Selenium and its redox speciation in rainwater from sites of Valparaíso region in Chile, impacted by mining activities of copper ores. Water Research 36, 115–122. https://doi.org/10.1016/S0043-1354(01)00240-8
Deboudt, K., Flament, P., Bertho, M.-L., 2004. Cd, Cu, Pb and Zn Concentrations in Atmospheric Wet Deposition at a Coastal Station in Western Europe. Water, Air, & Soil Pollution 151, 335–359. https://doi.org/10.1023/B:WATE.0000009906.55895.30
Delalieux, F., van Grieken, R., Potgieter, J.H., 2006. Distribution of Atmospheric Marine Salt Depositions over Continental Western Europe. Marine Pollution Bulletin 52, 606-11. https://doi.org/10.1016/j.marpolbul.2005.08.018
Di Tullo, P., 2015. Dynamique du cycle biogéochimique du sélénium en écosystèmes terrestres: rétention et réactivité dans le sol, rôle de la végétation. PhD Thesis. University of Pau.
Duce, R.A., Wasson, J.T., Winchester, J.W., Burns, F., 1963. Atmospheric Iodine, Bromine, and Chlorine. Journal of Geophysical Research 68, 3943. https://doi.org/10.1029/JZ068i013p03943
Floor, G.H., Iglesias, M., Roman-Ross, G., Corvini, P.F.X., Lenz, M., 2011. Selenium speciation in acidic environmental samples: Application to acid rain-soil interaction at Mount Etna volcano. Chemosphere 84, 1664–1670. https://doi.org/10.1016/j.chemosphere.2011.05.006
Fuge, R., 1987. Iodine in the Environment: Its Distribution and Relationship to Human Health. In: Hemphill, DD (Ed.), Trace Substances in Environmental Health-XXI. University of Missouri, Colombia, MO, pp. 74-87. http://inis.iaea.org/Search/search.aspx?orig_q=RN:19105067
Fuge, R., Johnson, C.C., 2015. Iodine and Human Health, the Role of Environmental Geochemistry and Diet, a Review. Applied Geochemistry 63, 282–302. https://doi.org/10.1016/j.apgeochem.2015.09.013
Gilfedder, B.S., Petri, M., Biester, H., 2007a. Iodine speciation in rain and snow: Implications for the atmospheric iodine sink. Journal of Geophysical Research: Atmospheres 112, D07301. https://doi.org/10.1029/2006JD007356
Gilfedder, B.S., Petri, M., Biester, H., 2007b. Iodine and bromine speciation in snow and the effect of orographically induced precipitation. Atmospheric Chemistry and Physics 7, 2661–2669. https://doi.org/10.5194/acp-7-2661-2007
Gilfedder, B.S., Lai, S.C., Petri, M., Biester, H., Hoffmann, T., 2008. Iodine speciation in rain, snow and aerosols. Atmospheric Chemistry and Physics 8, 6069–6084.
Ham, Y.-S., Tamiya, S., 2006. Selenium behavior in open bulk precipitation, soil solution and groundwater in alluvial fan area in Tsukui, Central Japan. Water Air & Soil Pollution 177, 45–57. https://doi.org/10.1007/s11270-005-9062-1
Hötzl, H., Rosner, G., Winkler, R., 1989. Long-Term Behaviour of Chernobyl Fallout in Air and Precipitation. Journal of Environmental Radioactivity 10, 157-71. https://doi.org/10.1016/0265-931X(89)90012-X
König, N., Kowalska, A., Brunialti, G., Ferretti, M., Clarke, N., Cools, N., Derome, J., Derome, K., De Vos, B., Fuerst, A., Jakovljevič, T., Marchetto, A., Mosello, R., O'Dea, P.,

Tartari, G.A., Ulrich, E., 2016. Part XVI: Quality Assurance and Control in Laboratories, In: UNECE, ICP Forests Programme Co-ordinating Centre (ed.): Manual on methods and criteria for harmonized sampling, assessment, monitoring and analysis of the effects of air pollution on forests. Thünen Institute of Forest Ecosystems, Eberswalde, Germany, 46 p. + Annex.

Låg, J., Steiness, E., 1974. Soil selenium in relation to precipitation. AMBIO A Journal of the Human Environment 3, 237-38.

Lawson, N.M., Mason, R.P., 2001. Concentration of Mercury, Methylmercury, Cadmium, Lead, Arsenic, and Selenium in the Rain and Stream Water of Two Contrasting Watersheds in Western Maryland. Water Research 35, 4039–4052. https://doi.org/10.1016/S0043-1354(01)00140-3

Lehto, J., Raty, T., Hou, X., Paatero, J., Aldahan, A., Possnert, G., Flinkman, J., Kankaanpaa, H., 2012. Speciation of I-129 in sea, lake and rain waters. Science of the Total Environment 419, 60–67. https://doi.org/10.1016/j.scitotenv.2011.12.061

Lequy, É., Conil, S., Turpault, M.-P., 2012. Impacts of Aeolian dust deposition on European forest sustainability: A review. Forest Ecology and Management 267, 240–252. https://doi.org/10.1016/j.foreco.2011.12.005

Lidman, F., Mörth, C.-M., Björkvald, L., Laudon, H., 2011. Selenium Dynamics in Boreal Streams: The Role of Wetlands and Changing Groundwater Tables. Environmental Science & Technology 45, 2677–2683. https://doi.org/10.1021/es102885z

Monahan-Pendergast, M.T., Przybylek, M., Lindblad, M., Wilcox, J., 2008. Theoretical Predictions of Arsenic and Selenium Species under Atmospheric Conditions. Atmospheric Environment 42, 2349-57. https://doi.org/10.1016/j.atmosenv.2007.12.028

Mosher, B.W., Duce, R.A., 1987. A global atmospheric selenium budget. Journal of Geophysical Research: Atmospheres 92, 13289–13298. https://doi.org/10.1029/JD092iD11p13289

Neal, C., Neal, M., Wickham, H., Hill, L., Harman, S., 2007. Dissolved iodine in rainfall, cloud, stream and groundwater in the Plynlimon area of mid-Wales. Hydrology and Earth System Sciences 11, 283–293. https://doi.org/10.5194/hess-11-283-2007

Pan, Y.P., Wang, Y.S., 2015. Atmospheric wet and dry deposition of trace elements at 10 sites in Northern China. Atmospheric Chemistry and Physics 15, 951–972. https://doi.org/10.5194/acp-15-951-2015

Pascaud, A., Sauvage, S., Coddeville, P., Nicolas, M., Croise, L., Mezdour, A., Probst, A., 2016. Contrasted spatial and long-term trends in precipitation chemistry and deposition fluxes at rural stations in France. Atmospheric Environment 146, 28–43. https://doi.org/10.1016/j.atmosenv.2016.05.019

Pio, C.A., Legrand, M., Oliveira, T., Afonso, J., Santos, C., Caseiro, A., Fialho, P., Barata, F., Puxbaum, H., Sanchez-Ochoa, A., Kasper-Giebl, A., Gelencser, A., Preunkert, S., Schock, M., 2007. Climatology of aerosol composition (organic versus inorganic) at nonurban sites on a west-east transect across Europe. Journal of Geophysical Research: Atmospheres 112, D23S02. https://doi.org/10.1029/2006JD008038

Pupier, J., Benedetti, L., Bouchez, C., Bourlès, D., Leclerc, E., Thiry, Y., Guillou, V., 2016. Monthly record of the Cl and ^{36}Cl fallout rates in a deciduous forest ecosystem in NE France in 2012 and 2013. Quaternary Geochronology 35, 26–35. https://doi.org/10.1016/j.quageo.2016.04.002

R Core Team, 2013. R: A language and Environment for Statistical Computing. R Foundation for Statistical Computing, Vienna, Austria.

Redon, P.-O., Abdelouas, A., Bastviken, D., Cecchini, S., Nicolas, M., Thiry, Y., 2011. Chloride and Organic Chlorine in Forest Soils: Storage, Residence Times, And

Influence of Ecological Conditions. Environmental Science & Technology 45, 7202-8. https://doi.org/10.1021/es2011918.

Reithmeier, H., Lazarev, V., Rühm, W., Schwikowski, M., Gäggeler, H.W., Nolte, E., 2006. Estimate of European ^{129}I Releases Supported by ^{129}I Analysis in an Alpine Ice Core. Environmental Science & Technology 40, 5891–5896. https://doi.org/10.1021/es0605725

Robberecht, H., Vangrieken, R., Vansprundel, M., Vandenberghe, D., Deelstra, H., 1983. Selenium in Environmental and Drinking Waters of Belgium. Science of the Total Environment 26, 163–172. https://doi.org/10.1016/0048-9697(83)90109-2

Roulier, M., Bueno, M., Coppin, F., Nicolas, M., Thiry, Y., Rigal, F., Pannier, F., Le Hécho, I., 2020. Atmospheric iodine, selenium and caesium depositions in France: II. Influence of forest canopies. Chemosphere. https://doi.org/10.1016/j.chemosphere.2020.128952.

Roulier, M., Bueno, M., Thiry, Y., Coppin, F., Redon, P.-O., Le Hécho, I., Pannier, F., 2018. Iodine distribution and cycling in a beech (Fagus sylvatica) temperate forest. Science of the Total Environment 645, 431–440. https://doi.org/10.1016/j.scitotenv.2018.07.039

Roulier, M., Coppin, F., Bueno, M., Nicolas, M., Thiry, Y., Della Vedova, C., Février, L., Pannier, F., Le Hécho, I., 2019. Iodine budget in forest soils: Influence of environmental conditions and soil physicochemical properties. Chemosphere 224, 20–28. https://doi.org/10.1016/j.chemosphere.2019.02.060

Saiz-Lopez, A., Plane, J.M.C., Baker, A.R., Carpenter, L.J., von Glasow, R., Gómez Martín, J.C., McFiggans, G., Saunders, R.W., 2012. Atmospheric Chemistry of Iodine. Chemical Reviews 112, 1773-1804. https://doi.org/10.1021/cr200029u

Sakata, M., Marumoto, K., Narukawa, M., Asakura, K., 2006. Regional variations in wet and dry deposition fluxes of trace elements in Japan. Atmospheric Environment 40, 521–531. https://doi.org/10.1016/j.atmosenv.2005.09.066

Suess, E., Aemisegger, F., Sonke, J.E., Sprenger, M., Wernli, H., Winkel, L.H.E., 2019. Marine versus Continental Sources of Iodine and Selenium in Rainfall at Two European High-Altitude Locations. Environmental Science & Technology 53, 1905–1917. https://doi.org/10.1021/acs.est.8b05533

Suzuki, Y., Sugimura, Y., Miyake, Y., 1981. The content of selenium and its chemical form in rain water and aerosol in Tokyo. Journal of the Meteorological Society of Japan. Journal of the Meteorological Society of Japan 50, 405–408.

Thimonier, A., Schmitt, M., Waldner, P., Schleppi, P., 2008. Seasonality of the Na/Cl ratio in precipitation and implications of canopy leaching in validating chemical analyses of throughfall samples. Atmospheric Environment 42, 9106–9117. https://doi.org/10.1016/j.atmosenv.2008.09.007

Truesdale, V.W., Jones, S.D., 1996. The variation of iodate and total iodine in some UK rainwaters during 1980–1981. Journal of Hydrology 179, 67–86. https://doi.org/10.1016/0022-1694(95)02873-0

Ulrich, E., Lelong, N., Lanier, M., Schneider, A., 1998. Regional Differences in the Relation Between Monthly Precipitation and Bulk Concentration in France (Renecofor). Water, Air, and Soil Pollution 102, 239-57. https://doi.org/10.1023/A:1004944828649.

Vidal, J.-P., Martin, E., Franchisteguy, L., Baillon, M., Soubeyroux, J.-M., 2010. A 50-year high-resolution atmospheric reanalysis over France with the Safran system. International Journal of Climatology 30, 1627–1644. https://doi.org/10.1002/joc.2003

Vriens, B., Lenz, M., Charlet, L., Berg, M., Winkel, L.H.E., 2014. Natural Wetland Emissions of Methylated Trace Elements. Nature Communications 5, 3035. https://doi.org/10.1038/ncomms4035

Wang, L., Tang, A., 2011. Oxidation Mechanisms of Dimethyl Selenide and Selenoxide in the Atmosphere Initiated by OH Radical. A Theoretical Study. Chemical Physics 382, 98-103. https://doi.org/10.1016/j.chemphys.2011.03.006

Wang, Z., Gao, Y., 2001. Biogeochemical cycling of selenium in Chinese environments. Applied Geochemistry 16, 1345–1351. https://doi.org/10.1016/S0883-2927(01)00046-4

Wen, H., Carignan, J., 2007. Reviews on atmospheric selenium: Emissions, speciation and fate. Atmospheric Environment 41, 7151–65. https://doi.org/10.1016/j.atmosenv.2007.07.035

Wen, H., Carignan, J., 2009. Ocean to Continent Transfer of Atmospheric Se as Revealed by Epiphytic Lichens. Environmental Pollution 157, 2790-97. https://doi.org/10.1016/j.envpol.2009.04.021.

Xu, S., Zhang, L., Freeman, S.P.H.T., Hou, X., Watanabe, A., Sanderson, D.C.W., Cresswell, A., Yamaguchi, K., 2016. Iodine isotopes in precipitation: Four-year time series variations before and after 2011 Fukushima nuclear accident. Journal of Environmental Radioactivity 155–156, 38–45. https://doi.org/10.1016/j.jenvrad.2016.02.011

Yudovich, Y.E., Ketris, M.P., 2006. Selenium in coal: A review. International Journal of Coal Geology 67, 112–126. https://doi.org/10.1016/j.coal.2005.09.003

Supporting Information

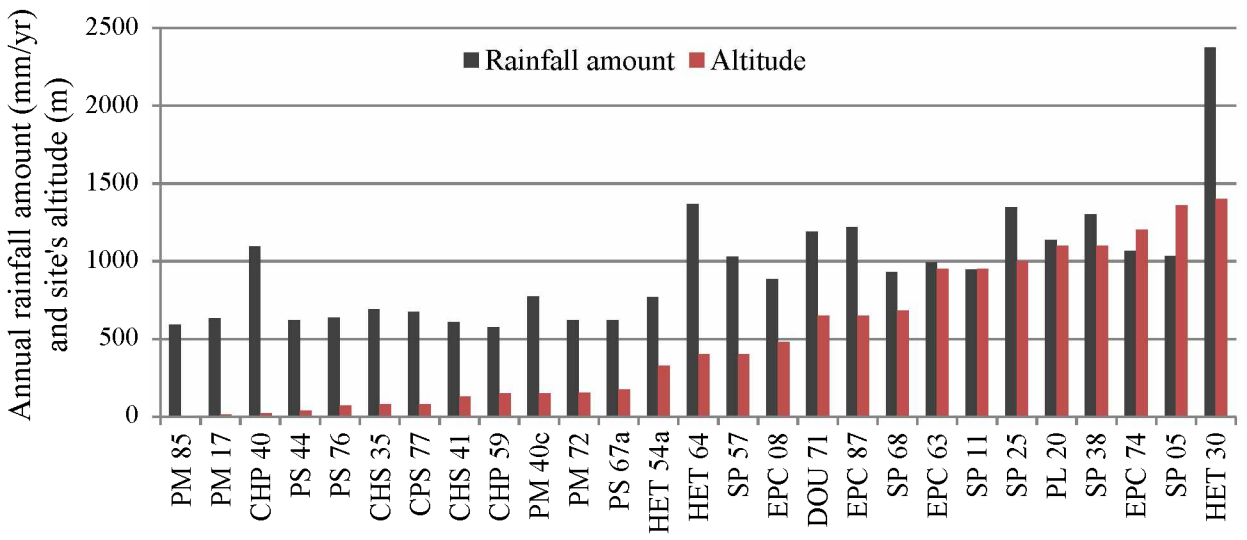

Figure S1. Annual rainfall amount in the study sites classified according to altitude (n = 27 sites).

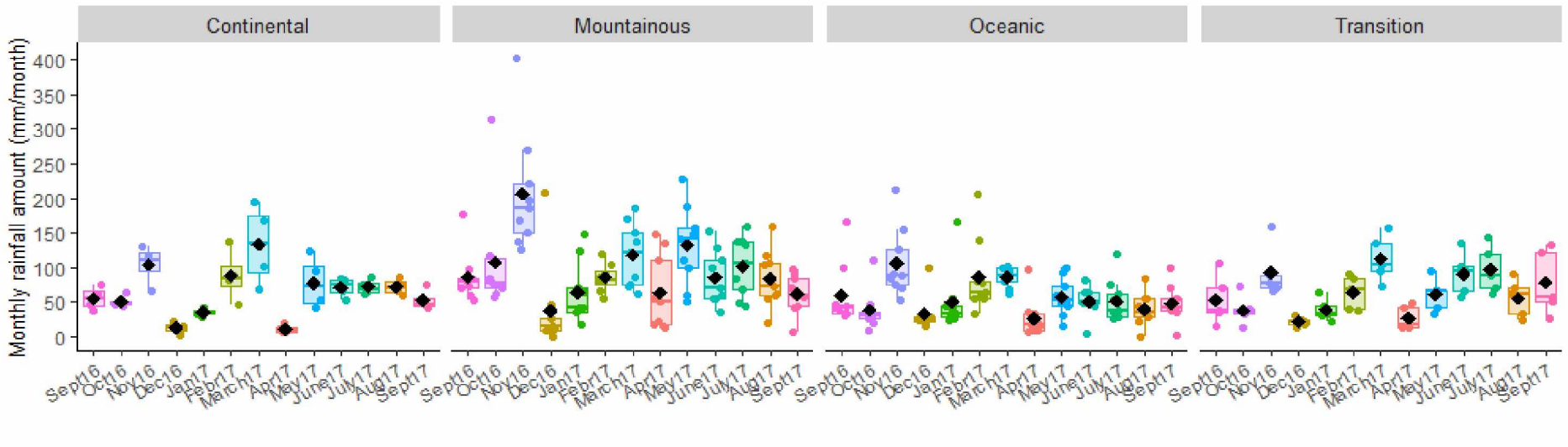

Figure S2. Boxplot distribution (distribution of data based on a five number summary: minimum, first quartile, median, third quartile and maximum) of monthly rainfall amount at the 27-study sites (grouped by climate). The Mediterranean site (PL20) is included in the Oceanic climate group. Black diamonds correspond to mean values.

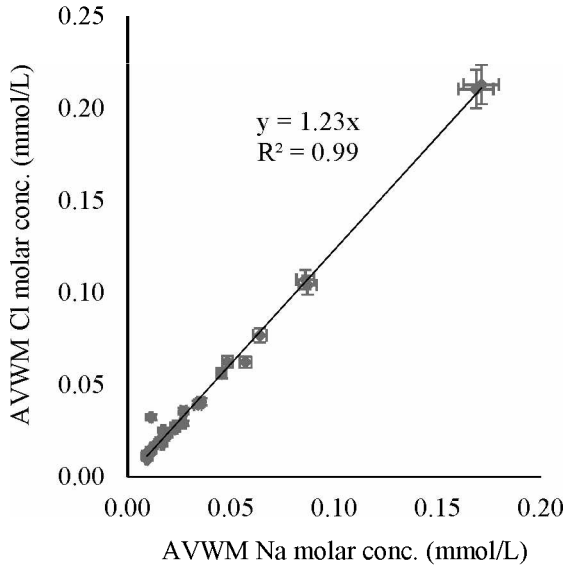

Figure S3. Molar AVWM Cl concentrations in rainfall as a function of those of Na (n = 27 sites). Error bars correspond to standard errors.

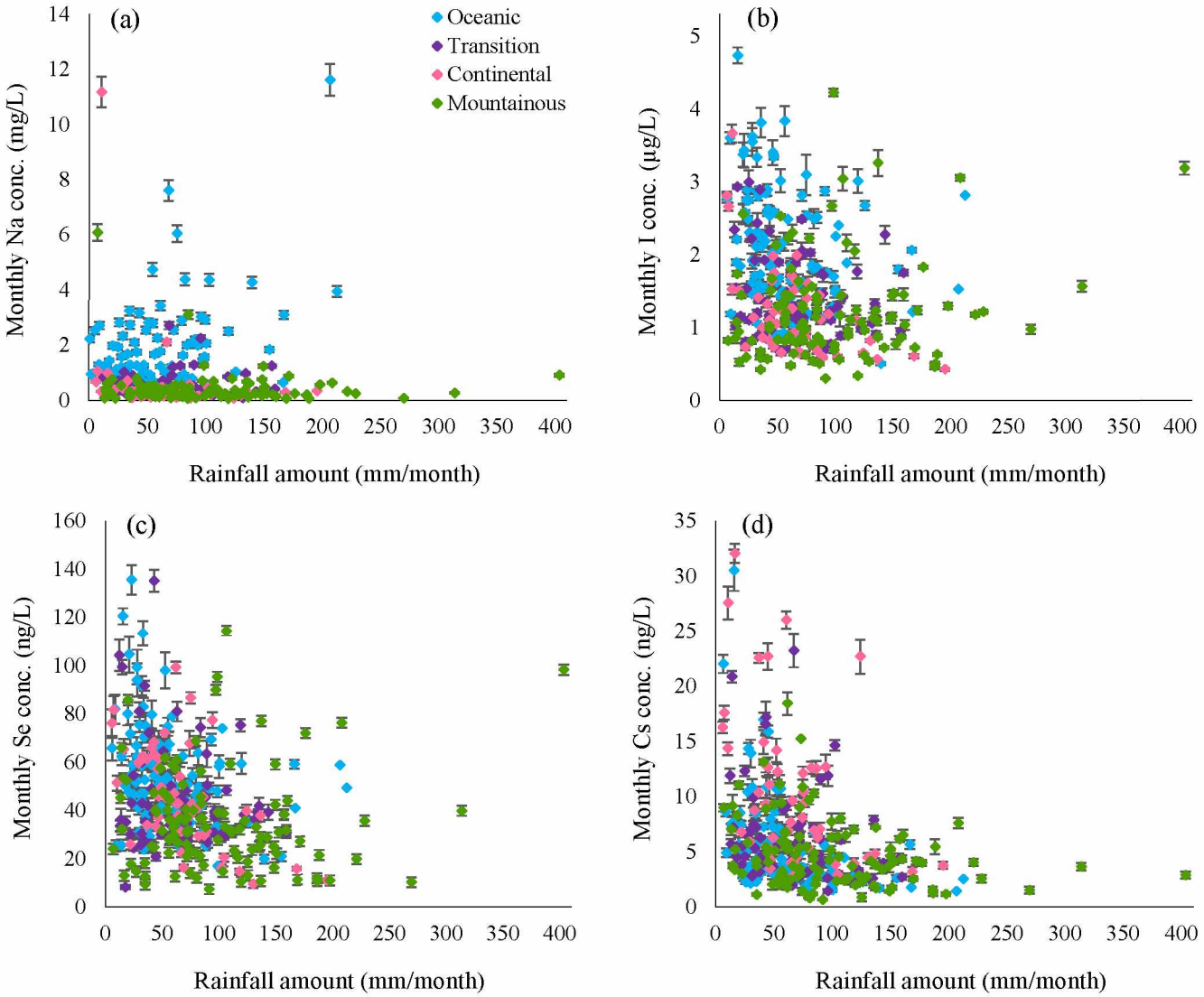

Figure S4. Monthly (a) sodium, (b) iodine, (c) selenium and (d) caesium concentrations in rainfall as a function of rainfall amount and according to climate. The Mediterranean site (PL20) is included in the Oceanic climate group. Error bars correspond to standard errors.

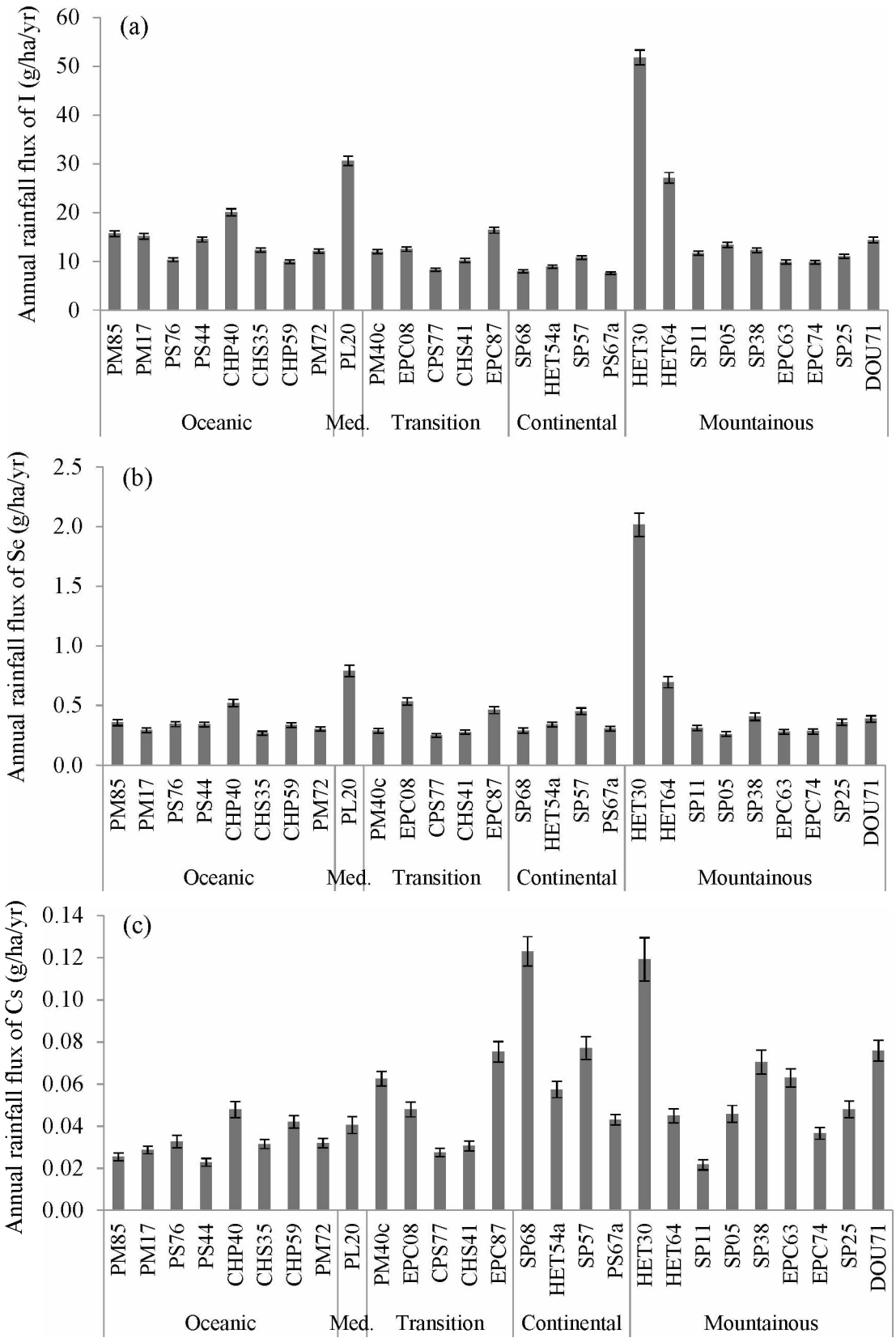

Figure S5. Annual rainfall fluxes of total (a) I, (b) Se and (c) Cs for the study sites, classified according to distance from coastsclimate (n = 27 sites). Med.: Mediterranean. Error bars correspond to standard errors. CHP: Pedunculate Oak; CHS: Sessile Oak; CPS: Pedunculate/Sessile Oak; HET: Beech; DOU: Douglas fir; EPC: Spruce; PS: Scots Pines; SP: Silver Fir.

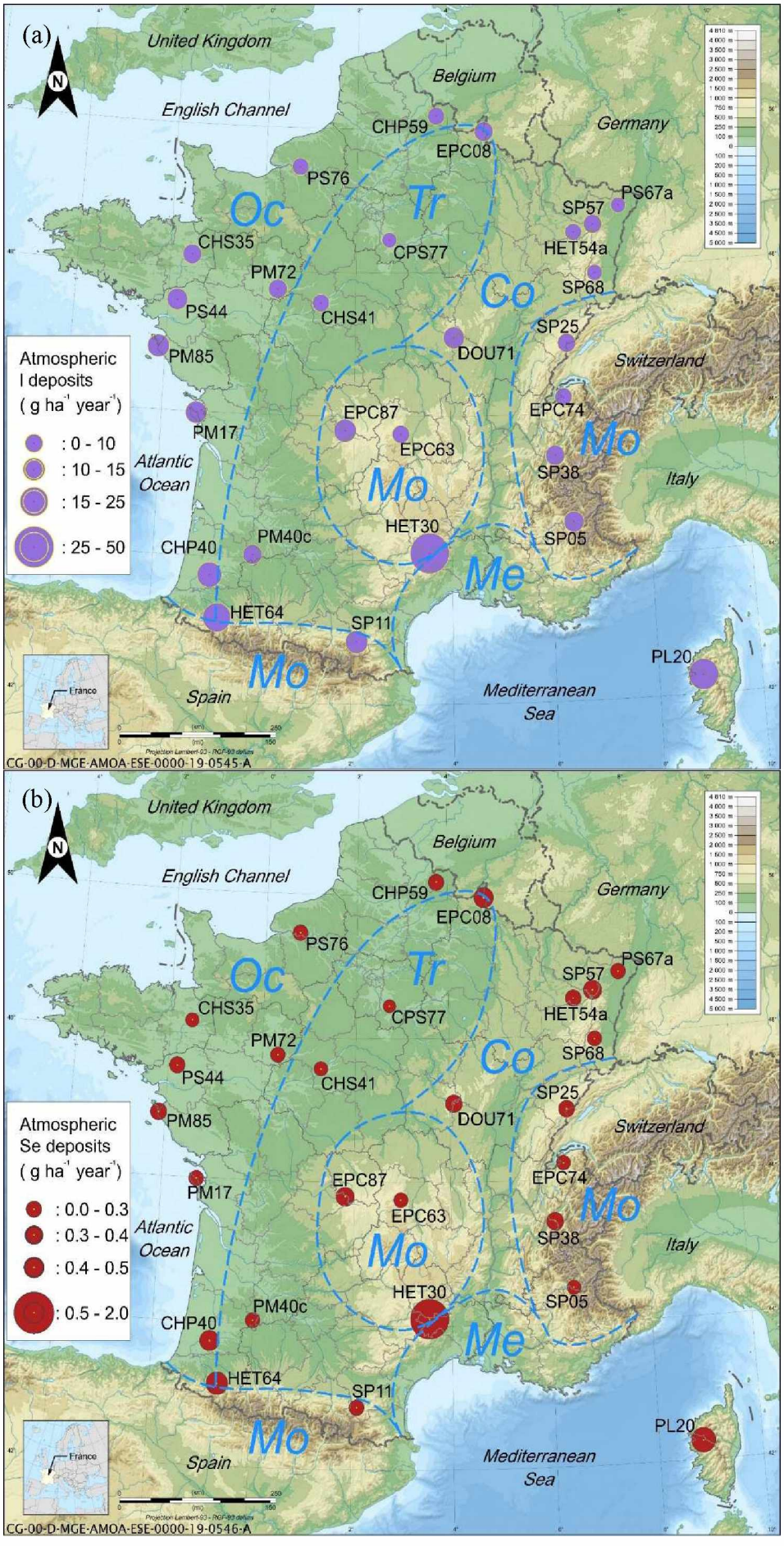
(a)
United Kingdom
Belgium
English Channel
Germany
CHP59
EPC08
PS76
PS67a
Oc
Tr
SP57
CHS35
CPS77
HET54a
PM72
Co
SP68
PS44
CHS41
SP25
PM85
DOU71
Switzerland
Atmospheric I deposits (g ha-1 year-1)
: 0 - 10
: 10 - 15
: 15 - 25
: 25 - 50
EPC87
EPC74
PM17
EPC63
Mo
Atlantic Ocean
SP38
Italy
Mo
HET30
PM40c
SP05
CHP40
Me
HET64
SP11
PL20
Mo
Spain
Mediterranean Sea
France
CG-00-D-MGE-AMOA-ESE-0000-19-0545-A
(b)
United Kingdom
Belgium
English Channel
Germany
CHP59
EPC08
PS76
PS67a
Oc
Tr
SP57
CHS35
CPS77
HET54a
PM72
Co
SP68
PS44
CHS41
SP25
PM85
DOU71
Switzerland
Atmospheric Se deposits (g ha-1 year-1)
: 0.0 - 0.3
: 0.3 - 0.4
: 0.4 - 0.5
: 0.5 - 2.0
EPC87
EPC74
PM17
EPC63
Mo
Atlantic Ocean
SP38
Italy
Mo
HET30
PM40c
SP05
CHP40
Me
HET64
SP11
PL20
Mo
Spain
Mediterranean Sea
France
CG-00-D-MGE-AMOA-ESE-0000-19-0546-A

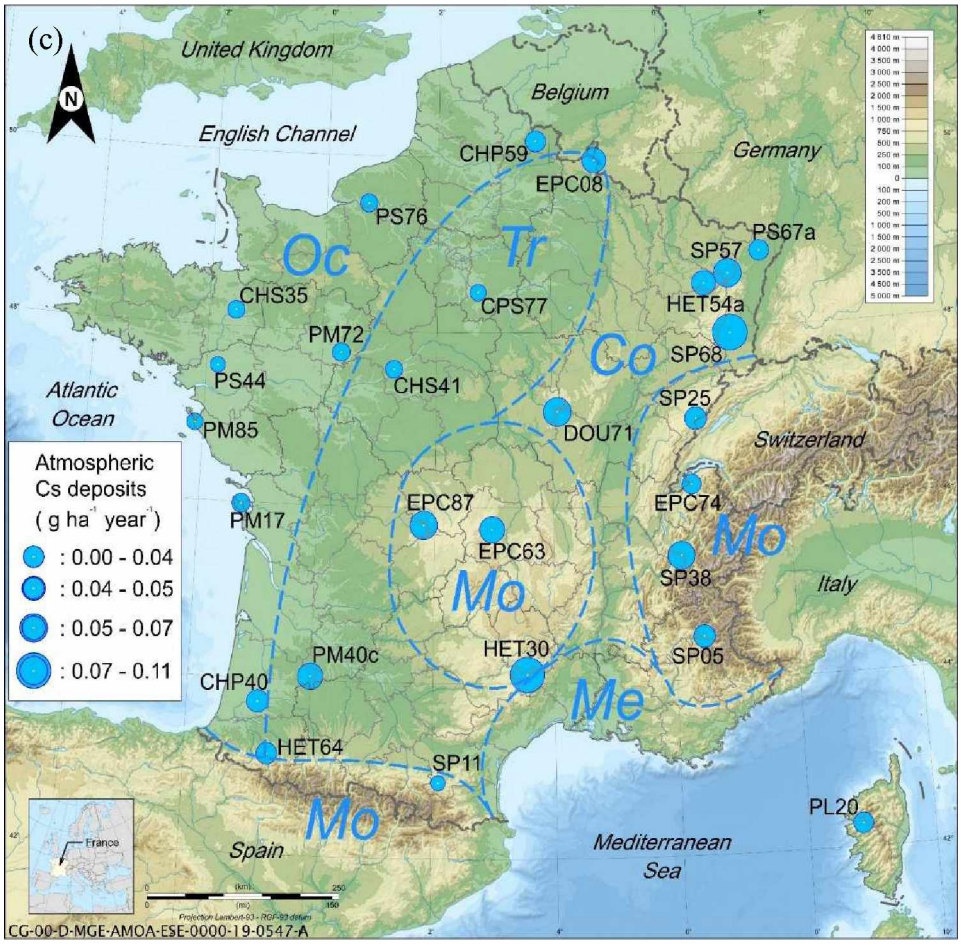

Figure S6. French climates and annual rainfall fluxes of (a) I, (b) Se and (c) Cs in studied sites (n = 27 sites). Period: September 2016 – September 2017. Oc: Oceanic; Tr: Transition; Co: Continental; Mo: Mountainous; Me: Mediterranean. Base map: Eric Gaba (https://commons.wikimedia.org/w/index.php?curid=4899458).

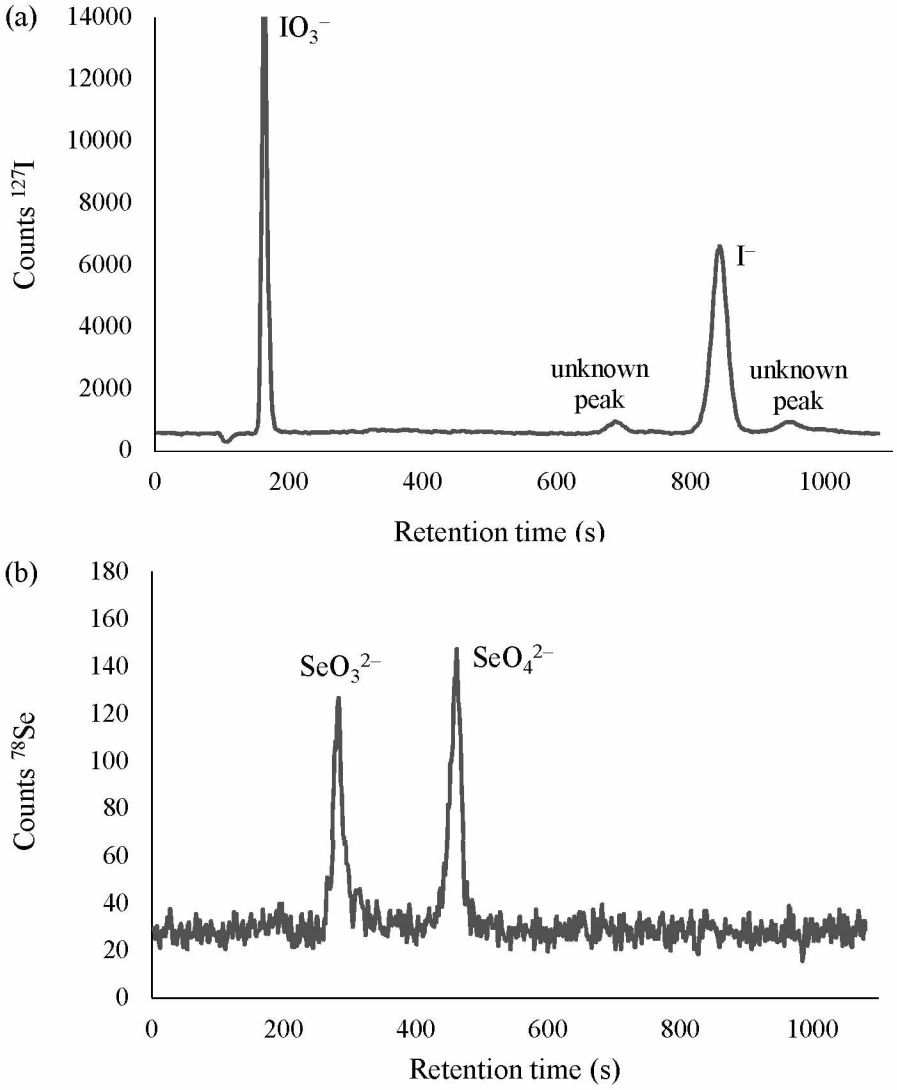

Figure S7. Example of IC-ICP-MS chromatograms of (a) inorganic iodine species and (b) inorganic selenium species in rainfall (sample EPC08, February 2017).

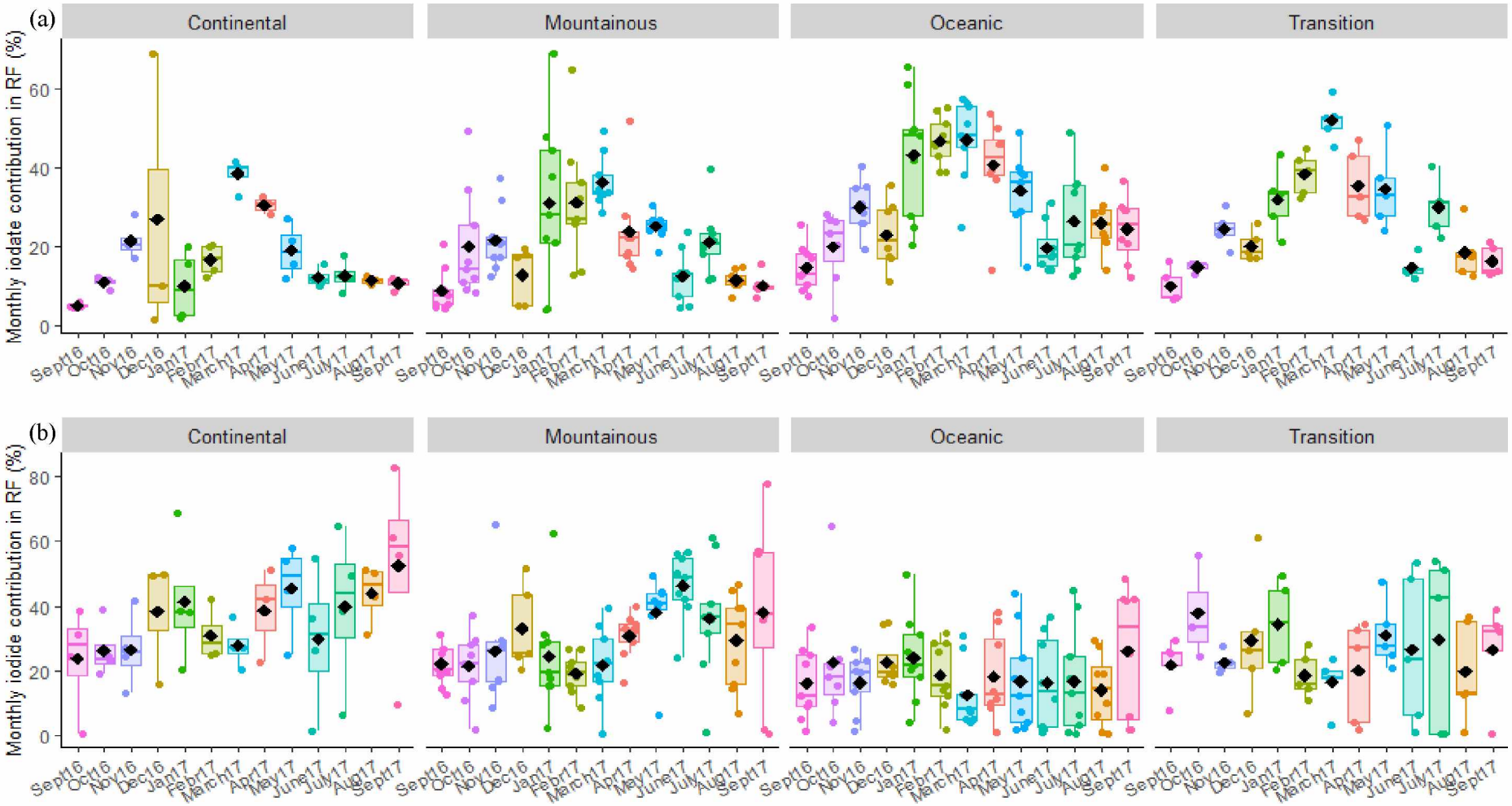
(a)
Continental
Mountainous
Oceanic
Transition
Monthly iodate contribution in RF (%)
0
20
40
60
Sept16
Oct16
Nov16
Dec16
Jan17
Febr17
March17
Apr17
May17
June17
July17
Aug17
Sept17
(b)
Continental
Mountainous
Oceanic
Transition
Monthly iodide contribution in RF (%)
0
20
40
60
80
Sept16
Oct16
Nov16
Dec16
Jan17
Febr17
March17
Apr17
May17
June17
July17
Aug17
Sept17

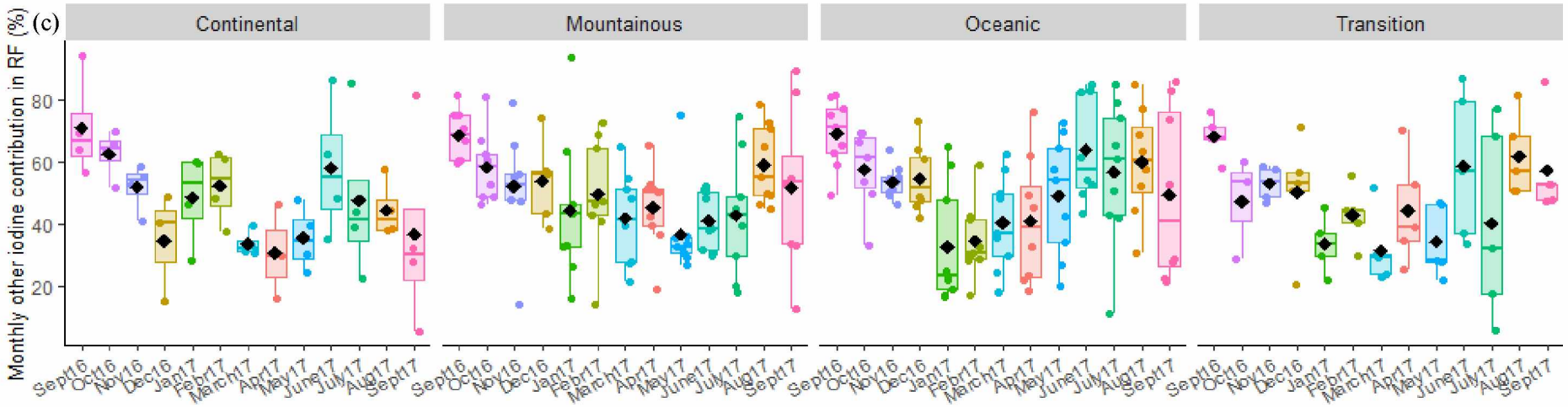

Figure S8. Boxplot distribution (distribution of data based on a five-number summary: minimum, first quartile, median, third quartile and maximum) of monthly (a) iodate, (b) iodide and (c) "other" iodine contributions in rainfall according to climate. The Mediterranean site (PL20) is included in the Oceanic climate group. Black dots correspond to mean values.

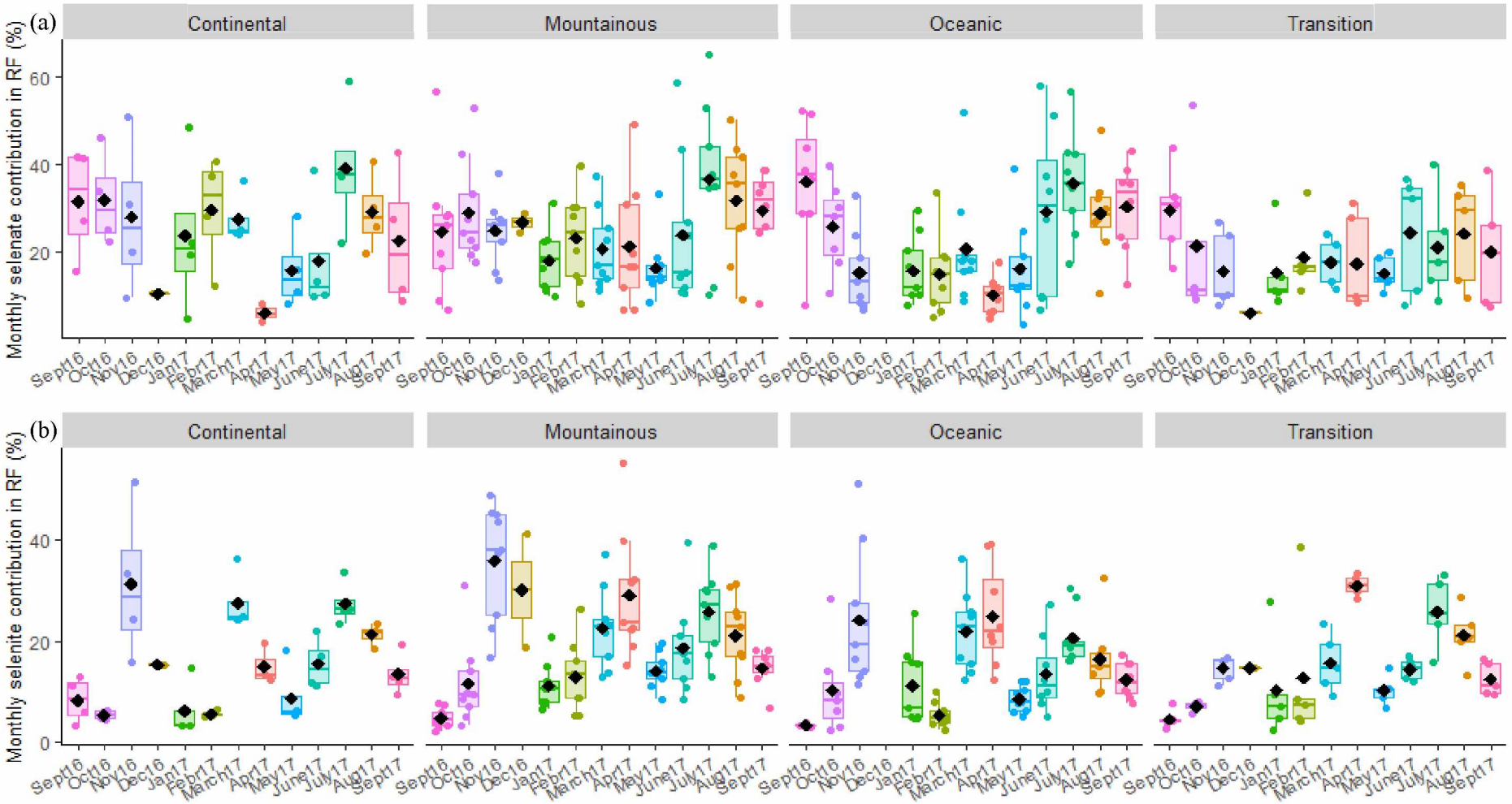
(a)
Continental
Mountainous
Oceanic
Transition
Monthly selenate contribution in RF (%)
0
20
40
60
Sept16
Oct16
Nov16
Dec16
Jan17
Fepr17
March17
Apr17
May17
June17
July17
Aug17
Sept17
(b)
Monthly selenite contribution in RF (%)

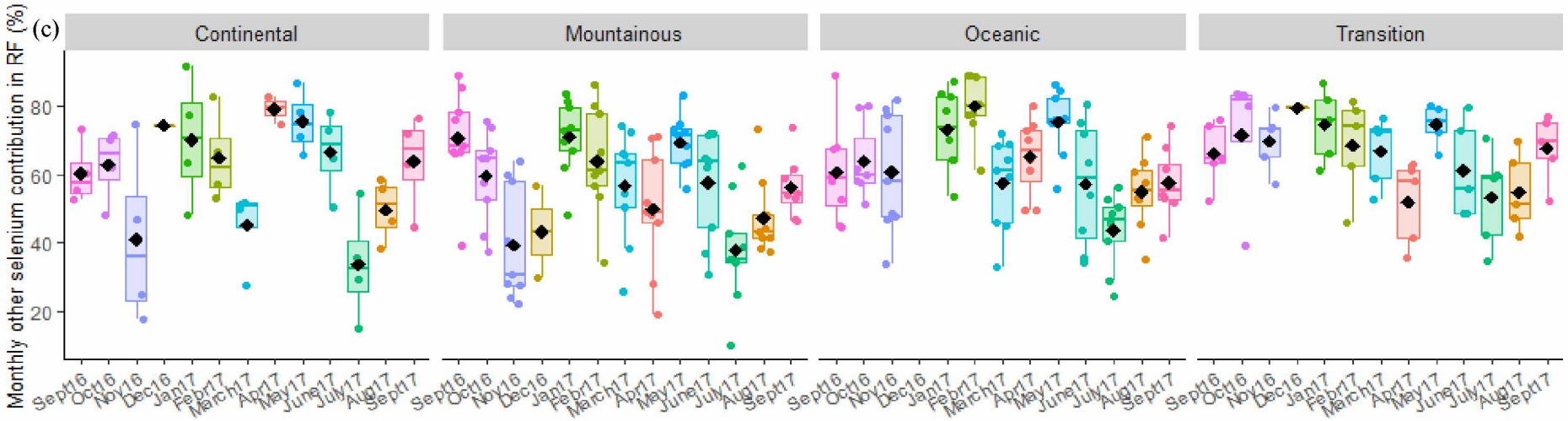

Figure S9. Boxplot distribution (distribution of data based on five number summary: minimum, first quartile, median, third quartile and maximum) of monthly (a) selenate, (b) selenite and (c) "other" selenium contribution in rainfall according to climate. The Mediterranean site (PL20) is included in the Oceanic climate group. Black dots correspond to mean value.

Table S1. Environmental characteristics of the study sites (n = 27 sites).

Forest site*	Dominant tree species*	Climate*
CHP40	Pedunculate Oak	Oceanic
CHP59	Pedunculate Oak	Oceanic
CHS35	Sessile Oak	Oceanic
CHS41	Sessile Oak	Transition
CPS77	Sessile/Ped. Oak	Transition
DOU71	Douglas-fir	Mountainous
EPC08	Spruce	Transition
EPC63	Spruce	Mountainous
EPC74	Spruce	Mountainous
EPC87	Spruce	Transition
HET30	Beech	Mountainous
HET54a	Beech	Continental
HET64	Beech	Mountainous
PL20	Black Pine	Mountainous/Med.
PM17	Maritime Pine	Oceanic
PM40c	Maritime Pine	Transition
PM72	Maritime Pine	Oceanic
PM85	Maritime Pine	Oceanic
PS44	Scots Pine	Oceanic
PS67a	Scots Pine	Continental
PS76	Scots Pine	Oceanic
SP05	Silver fir	Mountainous
SP11	Silver fir	Mountainous
SP25	Silver fir	Mountainous
SP38	Silver fir	Mountainous
SP57	Silver fir	Continental
SP68	Silver fir	Continental

: published in Redon et al. 2011

Table S2. Methods used for the determination of the main physicochemical properties of the rainwater. LQ: limit of quantification.

Parameter	Method	Standard	LQ (mg L^{-1})
pH	pH-Electrode	NF T 90 008	–
Cl^-	Ion chromatography	NF EN ISO 10304-1	0.1
NO_3^-			0.1
SO_4^{2-}			0.2
Na	ICP-AES	NF EN ISO 11885	0.01
Ca			0.01
Mg			0.001
K			0.05
$NH4^+$	Continous flow UV-VIS-spectrophotometry	NF EN ISO 11732	0.01
DOC	TOC/TN Analyzer	NF EN 1484	0.5
Total N		NF EN 12260	0.5

Table S3. ICP-MS operating conditions and data acquisition parameters for simultaneous total I and Cs concentration analysis (Agilent 7500ce) and for total Se concentration analysis (Agilent 7900).

ICP-MS	**Agilent 7500ce**	**Agilent 7900**
Sample introduction	Concentric nebulizer Scott spray chamber	Concentric nebulizer Scott spray chamber
Plasma parameters		
RF power	1500 W	1500 W
Ar plasma gas flow rate	15 L min^{-1}	15 L min^{-1}
Ar auxiliary gas flow rate	0.75-1.15 L min^{-1} optimized daily for best sensitivity[a]	0.75-1.15 L min^{-1} optimized daily for best sensitivity[a]
Sample and skimmer cones	Nickel	Nickel
Ions lens setting	Optimized daily for best sensitivity[a]	Optimized daily for best sensitivity[a,b]
Reaction/collision parameters		
H2 gas flow	–	5 mL min^{-1}
Octopole bias	-8 V	-18 V
Quadrupole bias	-6 V	-17 V
Data acquisition parameters		
Monitored isotopes	133, 127	77, 78
Acquisition time per point	0.1 s (0.3 s per peak)	0.2 s (0.6 s per peak)
Replicates	10	10

[a] Using a solution of 1 μg L^{-1} of gallium, yttrium, thallium and cerium + [b] cobalt and magnesium

Table S4. Annual water amount, mean pH and volume-weighted mean (AVWM) concentrations of dissolved organic carbon (DOC) in rainfall. Uncertainties correspond to standard errors.

Forest site	Water amount (mm yr^{-1})	pH			AVWM DOC concentration (mg L^{-1})		
CHP40	1093	5.6	±	0.5	0.39	±	0.02
CHP59	573	6.1	±	0.6	0.68	±	0.03
CHS35	691	6.0	±	0.3	0.64	±	0.03
CHS41	608	6.1	±	0.3	0.58	±	0.03
CPS77	673	6.0	±	0.3	0.50	±	0.03
DOU71	1189	6.2	±	0.3	0.39	±	0.02
EPC08	882	6.0	±	0.5	0.37	±	0.02
EPC63	993	6.2	±	0.4	0.25	±	0.01
EPC74	1067	6.2	±	0.3	0.31	±	0.02
EPC87	1218	5.8	±	0.2	0.40	±	0.02
HET30	2372	5.9	±	0.6	0.12	±	0.01
HET54a	769	6.4	±	0.3	0.66	±	0.03
HET64	1365	6.2	±	0.3	0.30	±	0.02
PL20	1134	6.4	±	0.7	0.07	±	0.00
PM17	633	6.1	±	0.3	0.52	±	0.03
PM40c	773	6.2	±	0.3	0.61	±	0.03
PM72	621	6.3	±	0.2	0.79	±	0.04
PM85	592	6.4	±	0.4	0.93	±	0.05
PS44	621	6.0	±	0.5	0.50	±	0.02
PS67a	619	6.2	±	0.7	0.61	±	0.03
PS76	637	5.8	±	0.5	0.61	±	0.03
SP05	1032	6.4	±	0.5	0.55	±	0.03
SP11	945	5.9	±	0.3	0.55	±	0.03
SP25	1347	6.1	±	0.4	0.33	±	0.02
SP38	1301	6.0	±	0.5	0.32	±	0.02
SP57	1029	5.6	±	0.5	0.41	±	0.02
SP68	931	5.7	±	0.4	0.27	±	0.01
Mean	***952***		***6.1***			***0.48***	
Median	***931***		***6.1***			***0.50***	
Min	***573***		***5.6***			***0.12***	
Max	***2372***		***6.4***			***0.93***	

Table S5. Annual volume-weighted mean (AVWM) concentrations of major elements in rainfall. Uncertainties correspond to standard errors.

Forest site	AVWM concentration (mg L^{-1})							
	Na	K	Mg	Ca	$N\text{-}NH_4$	Cl	$N\text{-}NO_3$	$S\text{-}SO_4$
CHP40	1.98 ± 0.10	0.20 ± 0.01	0.26 ± 0.01	0.51 ± 0.03	0.30 ± 0.02	3.80 ± 0.19	0.19 ± 0.01	0.38 ± 0.02
CHP59	0.62 ± 0.03	0.35 ± 0.02	0.12 ± 0.01	0.73 ± 0.04	0.73 ± 0.04	1.26 ± 0.06	0.38 ± 0.02	0.33 ± 0.02
CHS35	1.11 ± 0.06	0.21 ± 0.01	0.14 ± 0.01	0.34 ± 0.02	0.41 ± 0.02	2.21 ± 0.11	0.18 ± 0.01	0.24 ± 0.01
CHS41	0.53 ± 0.03	0.12 ± 0.01	0.07 ± 0.00	0.30 ± 0.01	0.41 ± 0.02	0.99 ± 0.05	0.24 ± 0.01	0.19 ± 0.01
CPS77	0.31 ± 0.02	0.13 ± 0.01	0.05 ± 0.00	0.47 ± 0.02	0.38 ± 0.02	0.63 ± 0.03	0.27 ± 0.01	0.19 ± 0.01
DOU71	0.39 ± 0.02	0.08 ± 0.00	0.05 ± 0.00	0.27 ± 0.01	0.42 ± 0.02	0.63 ± 0.03	0.21 ± 0.01	0.17 ± 0.01
EPC08	0.44 ± 0.02	0.08 ± 0.00	0.07 ± 0.00	0.36 ± 0.02	0.56 ± 0.03	0.79 ± 0.04	0.34 ± 0.02	0.26 ± 0.01
EPC63	0.26 ± 0.01	0.16 ± 0.01	0.05 ± 0.00	0.34 ± 0.02	0.46 ± 0.02	0.54 ± 0.03	0.21 ± 0.01	0.15 ± 0.01
EPC74	0.22 ± 0.01	0.14 ± 0.01	0.03 ± 0.00	0.54 ± 0.03	0.26 ± 0.01	0.41 ± 0.02	0.21 ± 0.01	0.16 ± 0.01
EPC87	0.53 ± 0.03	0.10 ± 0.01	0.07 ± 0.00	0.25 ± 0.01	0.25 ± 0.01	0.92 ± 0.05	0.18 ± 0.01	0.18 ± 0.01
HET30	0.62 ± 0.03	0.07 ± 0.00	0.09 ± 0.00	0.34 ± 0.02	0.29 ± 0.01	1.03 ± 0.05	0.26 ± 0.01	0.32 ± 0.02
HET54a	0.39 ± 0.02	0.36 ± 0.02	0.06 ± 0.00	0.45 ± 0.02	1.11 ± 0.06	0.89 ± 0.04	0.33 ± 0.02	0.29 ± 0.01
HET64	0.82 ± 0.04	0.11 ± 0.01	0.12 ± 0.01	0.50 ± 0.03	0.36 ± 0.02	1.45 ± 0.07	0.21 ± 0.01	0.28 ± 0.01
PL20	2.00 ± 0.10	0.21 ± 0.01	0.29 ± 0.01	0.89 ± 0.04	0.26 ± 0.01	3.69 ± 0.18	0.22 ± 0.01	0.45 ± 0.02
PM17	3.88 ± 0.19	0.27 ± 0.01	0.48 ± 0.02	0.70 ± 0.04	0.18 ± 0.01	7.46 ± 0.37	0.18 ± 0.01	0.50 ± 0.02
PM40c	1.04 ± 0.05	0.29 ± 0.01	0.16 ± 0.01	0.62 ± 0.03	0.30 ± 0.02	1.99 ± 0.10	0.22 ± 0.01	0.28 ± 0.01
PM72	0.78 ± 0.04	0.21 ± 0.01	0.09 ± 0.00	0.39 ± 0.02	0.50 ± 0.02	1.39 ± 0.07	0.26 ± 0.01	0.23 ± 0.01
PM85	3.94 ± 0.20	0.31 ± 0.02	0.57 ± 0.03	1.08 ± 0.05	0.27 ± 0.01	7.55 ± 0.38	0.18 ± 0.01	0.56 ± 0.03
PS44	1.47 ± 0.07	0.23 ± 0.01	0.19 ± 0.01	0.51 ± 0.03	0.39 ± 0.02	2.72 ± 0.14	0.21 ± 0.01	0.35 ± 0.02
PS67a	0.26 ± 0.01	0.24 ± 0.01	0.28 ± 0.01	1.93 ± 0.10	0.54 ± 0.03	1.15 ± 0.06	0.36 ± 0.02	0.74 ± 0.04
PS76	1.31 ± 0.07	0.20 ± 0.01	0.16 ± 0.01	0.46 ± 0.02	0.72 ± 0.04	2.21 ± 0.11	0.31 ± 0.02	0.42 ± 0.02
SP05	0.20 ± 0.01	0.15 ± 0.01	0.09 ± 0.00	1.39 ± 0.07	0.36 ± 0.02	0.44 ± 0.02	0.20 ± 0.01	0.24 ± 0.01
SP11	0.37 ± 0.02	0.08 ± 0.00	0.07 ± 0.00	0.44 ± 0.02	0.17 ± 0.01	0.73 ± 0.04	0.15 ± 0.01	0.18 ± 0.01
SP25	0.26 ± 0.01	0.10 ± 0.00	0.05 ± 0.00	0.45 ± 0.02	0.28 ± 0.01	0.46 ± 0.02	0.20 ± 0.01	0.20 ± 0.01
SP38	0.21 ± 0.01	0.17 ± 0.01	0.06 ± 0.00	0.46 ± 0.02	0.34 ± 0.02	0.36 ± 0.02	0.24 ± 0.01	0.19 ± 0.01
SP57	0.22 ± 0.01	0.09 ± 0.00	0.04 ± 0.00	0.26 ± 0.01	0.42 ± 0.02	0.47 ± 0.02	0.30 ± 0.01	0.17 ± 0.01
SP68	0.22 ± 0.01	0.07 ± 0.00	0.04 ± 0.00	0.27 ± 0.01	0.25 ± 0.01	0.34 ± 0.02	0.22 ± 0.01	0.14 ± 0.01
Mean	***0.90***	***0.18***	***0.14***	***0.56***	***0.40***	***1.72***	***0.24***	***0.29***
Median	***0.53***	***0.16***	***0.09***	***0.46***	***0.36***	***0.99***	***0.22***	***0.24***
Min	***0.20***	***0.07***	***0.03***	***0.25***	***0.17***	***0.34***	***0.15***	***0.14***
Max	***3.94***	***0.36***	***0.57***	***1.93***	***1.11***	***7.55***	***0.38***	***0.74***

Table S6. Annual volume-weighted mean (AVWM) concentrations of total iodine, selenium and caesium, and proportions of I and Se species in rainfall. Uncertainties correspond to standard errors.

Forest site	AVWM I conc. ($\mu g\ L^{-1}$)				AVWM Se conc. ($ng\ L^{-1}$)				AVWM Cs conc. ($ng\ L^{-1}$)
	I	I^- (%)	IO_3^- (%)	I_{other} (%)	Se	SeO_3^{2-} (%)	SeO_4^{2-} (%)	Se_{other} (%)	
CHP40	1.83 ± 0.07	16 ± 1	27 ± 1	57 ± 4	48 ± 3	9 ± 1	29 ± 2	62 ± 7	4.4 ± 0.3
CHP59	1.74 ± 0.07	19 ± 1	30 ± 2	51 ± 4	59 ± 4	13 ± 1	14 ± 1	74 ± 8	7.3 ± 0.5
CHS35	1.78 ± 0.06	11 ± 1	34 ± 2	56 ± 4	39 ± 3	14 ± 1	17 ± 2	69 ± 8	4.6 ± 0.3
CHS41	1.68 ± 0.06	21 ± 1	27 ± 1	52 ± 4	46 ± 3	8 ± 1	21 ± 2	72 ± 8	5.0 ± 0.4
CPS77	1.23 ± 0.05	25 ± 1	24 ± 1	51 ± 4	37 ± 3	9 ± 1	17 ± 2	74 ± 9	4.1 ± 0.3
DOU71	1.21 ± 0.05	34 ± 2	23 ± 1	43 ± 5	33 ± 2	11 ± 1	16 ± 2	73 ± 9	6.4 ± 0.4
EPC08	1.42 ± 0.05	27 ± 1	32 ± 2	41 ± 4	57 ± 4	10 ± 1	18 ± 2	72 ± 8	5.4 ± 0.4
EPC63	0.99 ± 0.04	31 ± 2	19 ± 2	50 ± 5	28 ± 2	11 ± 1	16 ± 1	73 ± 8	6.3 ± 0.4
EPC74	0.92 ± 0.04	31 ± 2	21 ± 1	48 ± 4	27 ± 2	11 ± 1	24 ± 2	65 ± 9	3.4 ± 0.3
EPC87	1.35 ± 0.05	34 ± 2	27 ± 1	39 ± 4	38 ± 2	10 ± 1	33 ± 3	57 ± 8	6.2 ± 0.4
HET30	2.18 ± 0.06	23 ± 1	17 ± 1	60 ± 4	85 ± 4	20 ± 2	34 ± 3	46 ± 6	5.0 ± 0.4
HET54a	1.16 ± 0.04	27 ± 2	16 ± 1	57 ± 4	44 ± 3	8 ± 1	17 ± 2	75 ± 8	7.5 ± 0.5
HET64	1.99 ± 0.08	25 ± 1	30 ± 1	44 ± 5	51 ± 3	6.9 ± 0.5	31 ± 2	62 ± 8	3.3 ± 0.2
PL20	2.70 ± 0.09	23 ± 1	32 ± 1	45 ± 4	70 ± 4	9 ± 1	26 ± 2	65 ± 7	3.6 ± 0.4
PM17	2.39 ± 0.10	24 ± 1	32 ± 2	44 ± 5	46 ± 3	9 ± 1	39 ± 3	52 ± 8	4.5 ± 0.3
PM40c	1.55 ± 0.06	16 ± 1	25 ± 1	59 ± 4	37 ± 2	9 ± 1	16 ± 1	75 ± 8	8.1 ± 0.4
PM72	1.95 ± 0.07	8.4 ± 0.5	26 ± 1	66 ± 4	49 ± 3	9 ± 1	21 ± 2	70 ± 8	5.2 ± 0.4
PM85	2.65 ± 0.10	20 ± 1	31 ± 2	48 ± 4	60 ± 4	11 ± 1	27 ± 2	62 ± 9	4.3 ± 0.3
PS44	2.34 ± 0.09	21 ± 1	37 ± 2	42 ± 4	55 ± 3	10 ± 1	22 ± 2	69 ± 8	3.7 ± 0.3
PS67a	1.23 ± 0.05	35 ± 2	19 ± 1	46 ± 4	49 ± 3	8 ± 1	37 ± 3	55 ± 8	6.9 ± 0.4
PS76	1.62 ± 0.06	20 ± 1	31 ± 1	49 ± 5	54 ± 3	13 ± 1	21 ± 2	67 ± 8	5.1 ± 0.5
SP05	1.30 ± 0.05	25 ± 1	21 ± 1	54 ± 5	23 ± 2	10 ± 1	20 ± 2	70 ± 9	4.1 ± 0.3
SP11	1.24 ± 0.05	26 ± 1	21 ± 1	53 ± 5	33 ± 2	8 ± 1	30 ± 3	62 ± 9	2.3 ± 0.3
SP25	0.82 ± 0.03	39 ± 2	20 ± 1	42 ± 5	27 ± 2	11 ± 1	15 ± 1	74 ± 9	3.6 ± 0.3
SP38	0.94 ± 0.04	30 ± 2	17 ± 1	53 ± 5	31 ± 2	10 ± 1	26 ± 2	64 ± 9	5.4 ± 0.4
SP57	1.05 ± 0.04	44 ± 2	16 ± 1	40 ± 4	44 ± 3	8 ± 1	21 ± 2	72 ± 7	7.5 ± 0.5
SP68	0.85 ± 0.03	33 ± 2	18 ± 1	49 ± 5	31 ± 2	11 ± 1	31 ± 3	58 ± 9	13.2 ± 0.8
Mean	***1.56***	***26***	***25***	***50***	***44***	***10***	***24***	***66***	***5.4***
Median	***1.42***	***25***	***25***	***49***	***44***	***10***	***21***	***69***	***5.0***
Min	***0.82***	***8***	***16***	***39***	***23***	***7***	***14***	***46***	***2.3***
Max	***2.70***	***44***	***37***	***66***	***85***	***20***	***39***	***75***	***13.2***

Table S7. Seasonal water amount and volume-weighted mean (SVWM) concentrations of total iodine in rainfall. Uncertainties correspond to standard errors. The four seasons were defined as follows: September 2016 to November 2016 and September 2017 (Autumn), December 2016 to February 2017 (Winter), March 2017 to May 2017 (Spring), and June 2017 to August 2017 (Summer).

Forest site	Water amount (mm season^{-1})				SVWM I conc. (μg L^{-1})			
	Autumn	Winter	Spring	Summer	Autumn	Winter	Spring	Summer
CHP40	389	188	287	229	2.00 ± 0.21	0.83 ± 0.14	1.42 ± 0.13	2.89 ± 0.26
CHP59	184	120	112	156	1.87 ± 0.19	1.46 ± 0.10	1.81 ± 0.30	1.53 ± 0.14
CHS35	201	126	178	186	2.54 ± 0.26	1.59 ± 0.17	1.33 ± 0.13	1.51 ± 0.13
CHS41	169	86	156	198	2.16 ± 0.20	1.13 ± 0.10	1.13 ± 0.10	1.67 ± 0.15
CPS77	275	96	150	152	1.42 ± 0.16	1.02 ± 0.09	0.97 ± 0.09	1.26 ± 0.14
DOU71	415	165	332	277	1.25 ± 0.13	1.00 ± 0.08	1.06 ± 0.09	1.45 ± 0.13
EPC08	260	177	190	256	1.40 ± 0.18	1.35 ± 0.13	1.62 ± 0.18	1.15 ± 0.10
EPC63	343	145	242	262	1.05 ± 0.11	0.90 ± 0.07	0.76 ± 0.07	1.06 ± 0.09
EPC74	362	135	218	352	0.97 ± 0.10	0.34 ± 0.03	0.68 ± 0.07	1.04 ± 0.10
EPC87	396	152	302	368	1.58 ± 0.15	0.82 ± 0.08	0.96 ± 0.08	1.63 ± 0.15
HET30	900	847	526	99	2.35 ± 0.20	2.22 ± 0.19	1.26 ± 0.11	1.42 ± 0.15
HET54a	261	130	162	216	1.42 ± 0.15	1.00 ± 0.11	0.90 ± 0.15	1.14 ± 0.10
HET64	456	248	308	353	2.36 ± 0.28	1.07 ± 0.11	1.18 ± 0.10	2.85 ± 0.25
PL20	425	472	197	41	2.06 ± 0.20	1.35 ± 0.12	2.43 ± 0.17	1.72 ± 0.09
PM17	204	115	162	152	2.63 ± 0.23	1.89 ± 0.18	1.69 ± 0.15	2.61 ± 0.22
PM40c	208	114	205	246	2.03 ± 0.20	0.99 ± 0.10	1.20 ± 0.10	1.69 ± 0.19
PM72	207	108	150	156	2.31 ± 0.26	1.98 ± 0.19	1.38 ± 0.12	1.98 ± 0.18
PM85	197	136	144	116	2.70 ± 0.23	2.36 ± 0.24	1.96 ± 0.18	3.40 ± 0.30
PS44	205	126	159	131	3.02 ± 0.31	1.70 ± 0.19	1.51 ± 0.17	2.87 ± 0.25
PS67a	234	86	116	183	1.43 ± 0.15	1.81 ± 0.20	1.00 ± 0.16	1.10 ± 0.10
PS76	255	126	144	113	1.67 ± 0.19	1.42 ± 0.13	1.63 ± 0.14	1.70 ± 0.20
SP05	491	97	243	201	1.35 ± 0.16	0.54 ± 0.04	1.04 ± 0.08	1.35 ± 0.12
SP11	317	221	245	162	1.60 ± 0.17	0.69 ± 0.07	0.83 ± 0.07	1.90 ± 0.17
SP25	471	174	362	340	0.82 ± 0.09	0.66 ± 0.06	0.71 ± 0.09	1.05 ± 0.10
SP38	401	171	338	391	1.09 ± 0.13	0.40 ± 0.03	0.73 ± 0.07	0.98 ± 0.08
SP57	300	201	281	247	1.26 ± 0.13	0.64 ± 0.06	0.81 ± 0.07	1.12 ± 0.10
SP68	256	129	330	217	1.00 ± 0.11	0.71 ± 0.06	0.55 ± 0.09	0.96 ± 0.09

Table S8. Seasonal volume-weighted mean (SVWM) concentrations of total selenium and caesium in rainfall. Uncertainties correspond to standard errors. The four seasons were defined as follows: September 2016 to November 2016 and September 2017 (Autumn), December 2016 to February 2017 (Winter), March 2017 to May 2017 (Spring), and June 2017 to August 2017 (Summer).

Forest site	SVWM Se conc. (ng L^{-1})				SVWM Cs conc. (ng L^{-1})			
	Autumn	Winter	Spring	Summer	Autumn	Winter	Spring	Summer
CHP40	47 ± 6	28 ± 4	47 ± 4	66 ± 7	5.0 ± 0.7	2.7 ± 0.4	4.7 ± 0.4	4.4 ± 0.7
CHP59	57 ± 6	78 ± 6	43 ± 7	57 ± 5	7.3 ± 0.8	7.7 ± 0.6	8.3 ± 1.6	6.0 ± 0.6
CHS35	52 ± 6	35 ± 4	33 ± 3	32 ± 3	5.9 ± 0.7	3.3 ± 0.4	3.4 ± 0.3	5.0 ± 0.4
CHS41	59 ± 6	37 ± 3	39 ± 3	36 ± 3	6.1 ± 0.5	4.3 ± 0.4	3.9 ± 0.4	4.5 ± 0.5
CPS77	38 ± 5	37 ± 3	36 ± 4	35 ± 3	3.9 ± 0.5	4.5 ± 0.4	4.8 ± 0.6	3.6 ± 0.4
DOU71	33 ± 4	31 ± 3	29 ± 3	37 ± 4	5.9 ± 0.7	5.3 ± 0.5	5.8 ± 0.6	8.5 ± 1.1
EPC08	45 ± 6	78 ± 7	65 ± 9	50 ± 4	4.2 ± 0.5	6.6 ± 0.6	6.5 ± 1.1	4.2 ± 0.4
EPC63	27 ± 3	24 ± 2	28 ± 3	28 ± 3	6.7 ± 0.8	4.1 ± 0.3	5.5 ± 0.5	6.8 ± 0.7
EPC74	24 ± 3	8 ± 1	27 ± 4	30 ± 3	2.3 ± 0.3	0.9 ± 0.1	3.4 ± 0.5	4.8 ± 0.4
EPC87	40 ± 4	23 ± 2	37 ± 3	43 ± 4	5.4 ± 0.7	4.4 ± 0.4	6.7 ± 0.7	7.3 ± 0.7
HET30	73 ± 6	111 ± 8	44 ± 4	40 ± 5	3.4 ± 0.3	6.3 ± 0.5	3.9 ± 0.4	5.8 ± 0.6
HET54a	51 ± 6	49 ± 5	37 ± 6	38 ± 3	6.0 ± 0.7	9.5 ± 1.7	7.9 ± 1.1	7.8 ± 0.7
HET64	53 ± 7	24 ± 3	33 ± 3	83 ± 8	3.3 ± 0.4	1.8 ± 0.2	2.9 ± 0.3	4.7 ± 0.5
PL20	45 ± 4	44 ± 4	76 ± 5	53 ± 3	3.9 ± 0.3	1.7 ± 0.2	3.5 ± 0.3	2.4 ± 0.1
PM17	40 ± 4	42 ± 4	44 ± 3	49 ± 5	2.7 ± 0.3	2.2 ± 0.2	5.3 ± 0.6	6.6 ± 0.8
PM40c	40 ± 4	34 ± 4	40 ± 3	35 ± 4	5.0 ± 0.5	5.5 ± 1.1	12.3 ± 1.4	8.4 ± 1.0
PM72	45 ± 6	49 ± 4	54 ± 4	48 ± 4	6.5 ± 0.9	3.5 ± 0.3	4.4 ± 0.4	5.3 ± 0.5
PM85	49 ± 4	57 ± 6	52 ± 5	82 ± 7	3.0 ± 0.3	2.3 ± 0.2	5.3 ± 0.6	6.6 ± 0.6
PS44	53 ± 6	67 ± 8	45 ± 5	59 ± 5	3.5 ± 0.4	2.5 ± 0.3	3.8 ± 1.1	4.9 ± 0.4
PS67a	52 ± 5	170 ± 24	37 ± 5	46 ± 4	5.3 ± 0.5	8.2 ± 0.8	8.8 ± 1.1	8.4 ± 0.8
PS76	51 ± 7	48 ± 4	54 ± 5	68 ± 7	5.0 ± 0.6	4.2 ± 0.4	6.0 ± 0.8	5.2 ± 0.5
SP05	18 ± 3	13 ± 1	26 ± 2	37 ± 3	2.8 ± 0.4	1.6 ± 0.3	3.5 ± 0.3	9.1 ± 0.9
SP11	32 ± 4	23 ± 3	29 ± 2	54 ± 5	2.4 ± 0.3	1.2 ± 0.2	2.2 ± 0.2	3.8 ± 0.4
SP25	25 ± 3	26 ± 2	25 ± 3	35 ± 3	2.7 ± 0.3	3.2 ± 0.5	3.7 ± 0.5	4.9 ± 0.4
SP38	28 ± 3	14 ± 1	26 ± 3	39 ± 3	3.4 ± 0.4	4.9 ± 0.7	6.3 ± 0.6	5.7 ± 0.5
SP57	46 ± 6	43 ± 4	38 ± 4	38 ± 3	7.7 ± 0.9	6.0 ± 0.6	6.7 ± 0.7	7.5 ± 0.7
SP68	24 ± 3	40 ± 3	23 ± 3	37 ± 3	11.7 ± 1.7	8.0 ± 0.6	11.7 ± 1.8	16.2 ± 1.6